IFM-GEOMAR REPORT

IFM-GEOMAR

Leibniz-Institut für Meereswissenschaften
an der Universität Kiel

RV POSEIDON
Fahrtbericht / Cruise Report P395
Sahara Slide Complex

04.02. – 19.02.2010
Las Palmas - Las Palmas (Spain)

Berichte aus dem Leibniz-Institut
für Meereswissenschaften an der
Christian-Albrechts-Universität zu Kiel

Nr. 50

November 2011

IFM-GEOMAR
Leibniz-Institut für Meereswissenschaften
an der Universität Kiel

RV POSEIDON
Fahrtbericht / Cruise Report P395
Sahara Slide Complex

04.02. – 19.02.2010
Las Palmas - Las Palmas (Spain)

Berichte aus dem Leibniz-Institut
für Meereswissenschaften an der
Christian-Albrechts-Universität zu Kiel

Nr. 50
November 2011

ISSN Nr.: 1614-6298

IFM-GEOMAR
Leibniz-Institut für Meereswissenschaften
an der Universität Kiel

Das Leibniz-Institut für Meereswissenschaften
ist ein Institut der Wissenschaftsgemeinschaft
Gottfried Wilhelm Leibniz (WGL)

The Leibniz-Institute of Marine Sciences is a
member of the Leibniz Association
(Wissenschaftsgemeinschaft Gottfried
Wilhelm Leibniz).

Herausgeber / Editor:
S. Krastel

IFM-GEOMAR Report
ISSN Nr.: 1614-6298

Leibniz-Institut für Meereswissenschaften / Leibniz Institute of Marine Sciences
IFM-GEOMAR
Dienstgebäude Westufer / West Shore Building
Düsternbrooker Weg 20
D-24105 Kiel
Germany

Leibniz-Institut für Meereswissenschaften / Leibniz Institute of Marine Sciences
IFM-GEOMAR
Dienstgebäude Ostufer / East Shore Building
Wischhofstr. 1-3
D-24148 Kiel
Germany

Tel.: ++49 431 600-0
Fax: ++49 431 600-2805
www.ifm-geomar.de

Contents

1. Summary

The main objective of Poseidon cruise P395 was to investigate the headwall area of the large Sahara Slide complex. The Sahara Slide complex is a mega slide with a length of ~900 km and an estimated volume of ~600 km^3. The age of the main slide event is 50-60 ka. The distal part of this slide complex is well studied, while data density in the source-area was sparse prior to Poseidon cruise P395. New data of the headwall area were collected during a 16-day cruise by means of a deep-towed side scan sonar, bathymetric mapping, and seismic profiling in February 2010. Gravity cores were taken based on the acoustic data. Bathymetric and side scan data reveal a slab type failure with multiple headwalls spanning ~35 km along slope in 1900 m water depth. The stacked headwalls are associated with at least three different glide planes. Some areas are characterized by elongated blocks, which have not moved far, while other areas are characterized by quickly disintegrating sediment masses. Seismic data show older mass transport deposits and giant downslope striking mound-like features, which are aligned with the sidewalls. Gravity cores taken beneath the upper headwall complex suggest an age of only 1 – 2 ka for this major failure. This age may represent a major re-activation of an existing headwall or a major failure of undisturbed slope sediments. The young age of this slide calls for a re-assessment of the risk potential of this margin.

Zusammenfassung

Das Hauptaugenmerk der Poseidon Fahrt P395 lag auf der Untersuchung der Abrisskante des großen Sahara-Rutschungs-Komplexes. Diese gigantische Massenbewegung befindet sich am passiven Kontinentalhang vor der Küste West Saharas und besitzt eine Länge von mehr als 900 km. Circa 600 km^3 an Sedimenten wurden durch diesen Prozess mobilisiert und umgelagert. Das Hauptalter der Rutschung beträgt 50-60.000 Jahre. Während der Ablagerungsbereich der Rutschungssedimente sehr gut untersucht ist, existierten von der Abrisskante vor der Poseidon Fahrt P395 nur sehr wenige Daten. Im Rahmen der 16-tägigen Fahrt im Februar 2010 wurden hydroakustische Daten (Seismik, Sidescan Sonar, Sediment-Echolot und Fächerecholot) gesammelt, die als Grundlage für die geologische Beprobung mittels Schwerelot dienten. Bathymetrische und Sidescan Sonar Daten zeigen mehrere Abrisskanten mit einer Gesamtlänge von ~35 km in ca. 1900 m Wassertiefe. Rutschungsflächen wurden in drei unterschiedlichen Tiefen identifiziert. Einige Bereiche unterhalb der Abrisskante zeigen längliche Blöcke, die nicht weit gerutscht sind, während andere Bereiche durch schnell zerfallende Sedimentmassen gekennzeichnet sind. Seismische Daten zeigen Ablagerungen älterer Massenbewegungen und sehr große Kämme, die hangabwärts streichen und mit der Lage der Seitenkanten der Rutschung übereinstimmen. Schwerelote, die direkt unterhalb der Abrisskante gewonnen wurden, deuten ein sehr junges Alter von nur 1000 – 2000 Jahren des letzten Kollapses an. Dieses Alter kann ein große Reaktivierung einer bestehenden Abrisskante oder den Kollaps von ungestörten Hangsedimenten repräsentieren. Das junge Alter des letzten Rutschungereignisses erfordert eine Neubewertung des Gefahrenpotentials des NW-Afrikanischen Kontinentalhanges.

2. Participants

Name	Discipline	Institution
Krastel, Sebastian, Prof. Dr.	Chief Scientist	IFM-GEOMAR
Georgiopoulou, Aggeliki, Dr.	Acoustics	UCD
Golbeck, Inga	Acoustics	GeoB
Grün, Matthias	Acoustics	IFM-GEOMAR
Klaucke, Ingo, Dr.	Side scan Sonar	IFM-GEOMAR
Mayer Mathias	Seismcis	IFM-GEOMAR
Schott, Thorsten	Technician	OKTOPUS
Vallée, Maxlimer	Acoustics	IFM-GEOMAR
Winkelmann, Daniel, Dr.	Sedimentology	IFM-GEOMAR
Wynn, Russel B., Dr.	Sedimentology	NOCS

Participating Institutions:

IFM-GEOMAR	*Leibniz Institute of Marine Sciences (IFM-GEOMAR), Kiel, Germany*
UCD	*School of Geological Sciences, University College Dublin, Ireland*
GeoB	*Fachbereich Geowissenschaften, Universität Bremen, Germany*
OKTOPUS	*Oktopus GmbH, Kiel, Germany*
NOCS	*National Oceanography Centre, Southampton, UK*

3. Objectives of the cruise

Submarine landslides present a major natural hazard, as they can destroy offshore infrastructures and may create destructive tsunamis. The NW-African continental margin is characterized by a complex interplay between gravitational and contour parallel sediment transport processes including large scale mass wasting at several locations. The Sahara Slide Complex is one of the giant landslides along the NW-African continental margin. This slide is well investigated in its distal depositional part (Embley 1976; Masson et al. 1993; Gee et al. 1999) but less was known about the headwall area. Hence Cruise P395 aimed in collecting detailed acoustic data and sediment cores from the headwall area in order to analyze the Sahara Slide complex from 'source-to-sink'. The slide can act as end member for mega-slides at passive, non-glaciated margins

3.1.The northwest African continental margin

The northwest African continental margin is a passive margin and large earthquakes are rare although moderate magnitude earthquakes have been recorded and are attributed to old zones of weakness created during the opening of the Atlantic Ocean (Hayes and Rabinowitz, 1975). Continental slope gradients range from 1° to 6°, while the continental rise displays gradients of <1° (Masson et al., 1992). South of 35° N sediment accumulation on the continental margin is driven by coastal upwelling creating sediments with elevated biogenic content, while fluvial inputs remain apparently low (Weaver et al., 2000).The upwelling cells give rise to high accumulation rates along the upper slope and shelf edge. Megaturbidites derived from this margin and deposited on the Madeira Abyssal plain are characterized by their high organic contents (0,5 to 2 %; Masson et al., 1992), suggesting that the upwelling derived sediment is potentially unstable, presumably as result of slope over-steepening. Furthermore, the Canary Islands contribute volcaniclastic material in this area through both large-scale landsliding (Masson et al., 2002; Wynn et al., 2002) as well as slow fallout through the water column into hemipelagic sediments. To the south of the Canary Islands, off Western Sahara and northern Mauritania, the continental margin is dominated by hemipelagic sediments and large open-slope landslides, in particular the giant Mauritania, Cap Blanc and Sahara Slides (Embley, 1982; Gee et al., 1999; Wynn et al., 2000; Krastel et al., 2006; Georgiopoulou et al., 2007).

Most of the northwest African continental margin south of 26°N is subject to large scale mass movement, giving rise to debris flow and turbidity currents. The turbidity currents transverse the slope and deposits thick layers on the abyssal plain, while debris flows deposits on the continental slope and rise (Weaver et al., 2000). A map of the main sedimentary features on the East Atlantic margin is shown in Fig. 1.

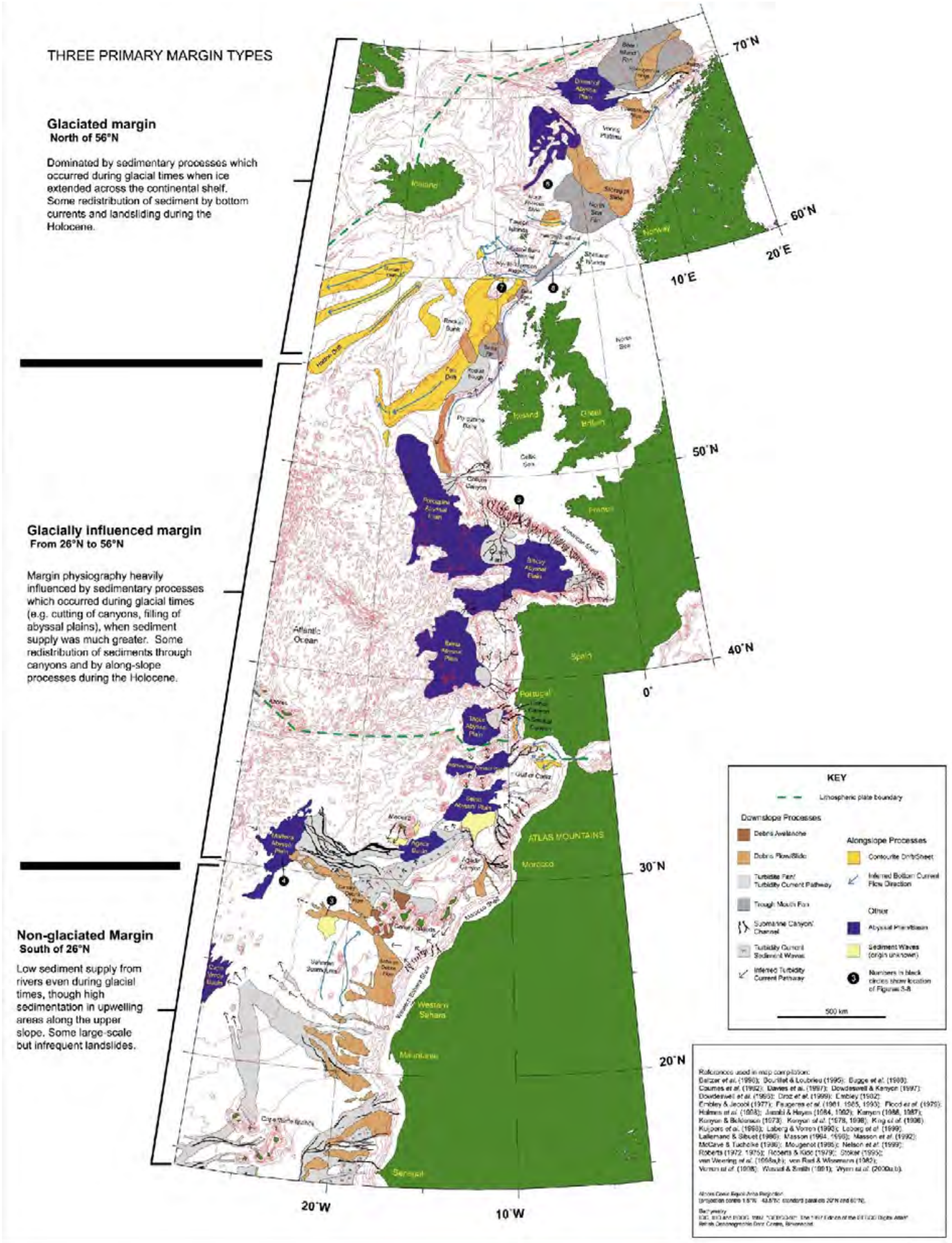

Fig. 1: Map of the main sedimentary features on the northeast Atlantic margin. The bottom part of the map shows down slope processes off the northwest African margin. Debris flow (light brown), debris avalanche (darker brown), turbidity currents pathway (light grey) (Weaver et al., 2000).

3.2.The Sahara Slide Complex

The oldest reference to the Sahara Slide dates back to 1977, when Embley and Jacobi (1977) describe it as the largest slide so far discovered with a slide scar of 18.000 km^2 in area and at least 600 km^3 in volume of translated Neogene sediments.

Gee et al. (1999) described the Sahara Debris Flow as a two-phase flow event, with a basal volcaniclastic layer and an overlying pelagic layer, which travelled for more than 400 km on a highly fluid, low friction layer of poorly sorted sediments (Fig. 3, Fig. 2). Regarding to the deposition of the debris flow Gee et al. (1999) conclude that it might have been controlled by a variety of factors, including decreasing gradients, thinning of the flow, and dissipation of pore pressure. Additionally, the age of the Sahara Slide was determined by examining the distal deposits of the Sahara Slide deposit resulting in an age of ~ 60 ka for the mass movement.

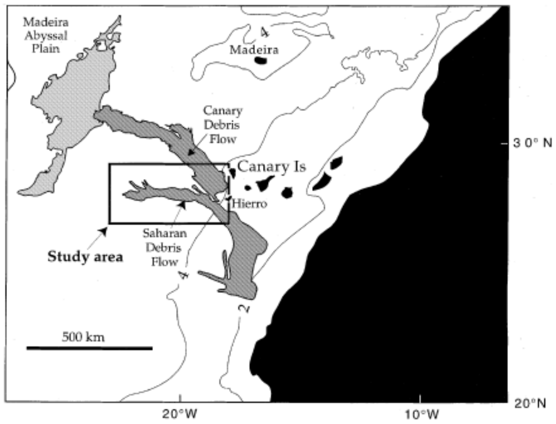

Fig. 3: Location of the Sahara Slide complex on the NW African continental margin to the South of the Canary Island. Contours are in kilometers below sea level (Gee et al., 1999)

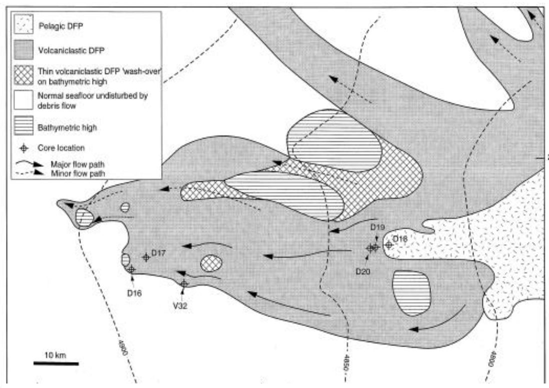

Fig. 2: Detailed map of the debris flow tongue showing relationships between the terminations of the pelagic and volcaniclastic debris flow phases and their interactions with the sea floor topography. Contour interval is 50 m (Gee el al., 1999).

Georgiopoulou et al. (2007) found that the headwall area has been the site of numerous massive landslides since at least Miocene times, as recorded by multiple buried events. They showed that landsliding has been taking place retrogressively and proposed differential compaction across buried scarps as the main preconditioning factor driving repeated instability (Fig. 4,Fig. 5).

Georgiopoulou et al. (2009) presented evidence for further sliding in the headwall area, occurring as recently as the Late Holocene. They showed that this 1 to 2 ka old event is related to a linked debrite-turbidite deposit, found further down slope and a surficial turbidite deposit covering a large area of the northwest African margin.

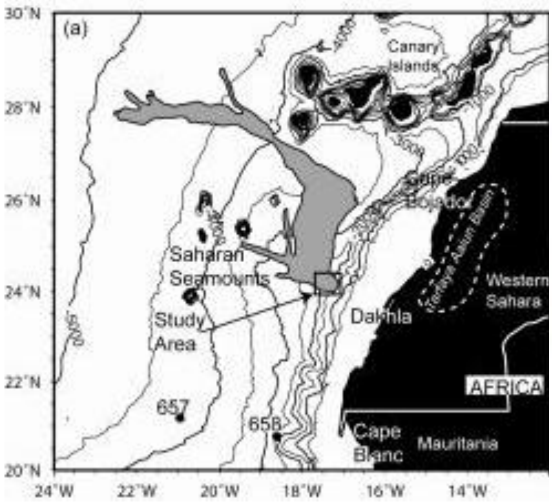

Fig. 4: Location of the study area by Georgiopolou et al., (2007) on the NW African margin (box). Map showing the outline of the Sahara Slide (grey-shaded area). Contours are at 500 m.

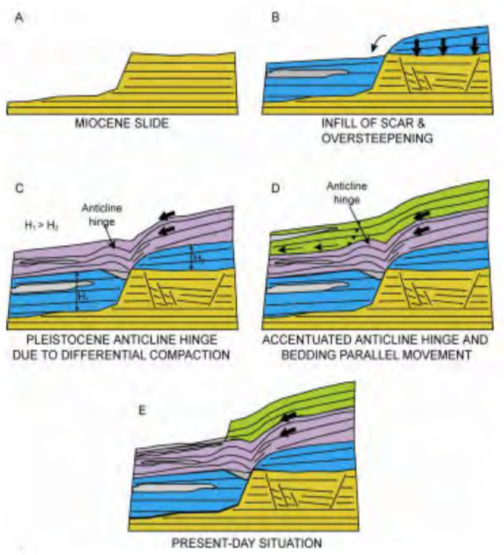

Fig. 5: Conceptual model of slide generation due to buried scarps (not to scale) (Georgiopolou et al., 2007).

3.3.Research Program

The morphology and evolution of the headwall area of the Sahara Slide complex was studied during a 16-day research cruise with RV Poseidon by means of deep-towed side scan sonar, bathymetric mapping, and seismic profiling in February 2010 (Fig. 6). Individual slide masses as well as undisturbed sediments upslope of the headwall were sampled by gravity coring in order to investigate trigger mechanisms and present day slope stability. The investigations shall lead to a detailed analysis of flow processes of the Sahara Slide complex from source to sink. The investigations are related to the project B4 (Submarine hazards at continental margins) within the Cluster of Excellence 'The Future Ocean', University of Kiel and Leibniz Institute of Marine Sciences (IFM-GEOMAR).

Specific objectives of the cruise were:

- *Analysis of the morphology and architecture of the headwall area*
  Detailed morphological maps of the scar area showing the location of individual headwalls and slide units were not available prior to the cruise.
- *Investigation of relatively recent reactivations of the headwall area and current slope stability*
  A pilot study indicated a young reactivation of the headwall but size and exact age were unknown.
- *Evaluation of possible triggers*
  Based on a single seismic line, Georgiopolou et al. (2007) postulated differential compaction over buried scarps as main trigger mechanism for the Sahara Slide complex. The new data allow to test this hypothesis due to a dense net of seismic profiles.

- *Assessment of associated geohazards*
  Recurrence rates and size of individual events are essential in order to assess the geohazard potential
- Synthesis of the Sahara Slide from 'Source-to-Sink'
  The new data should lead to an analysis of the Sahara Slide complex from 'source-to-sink'. The slide can act as end member for mega-slides at passive, non-glaciated margins.

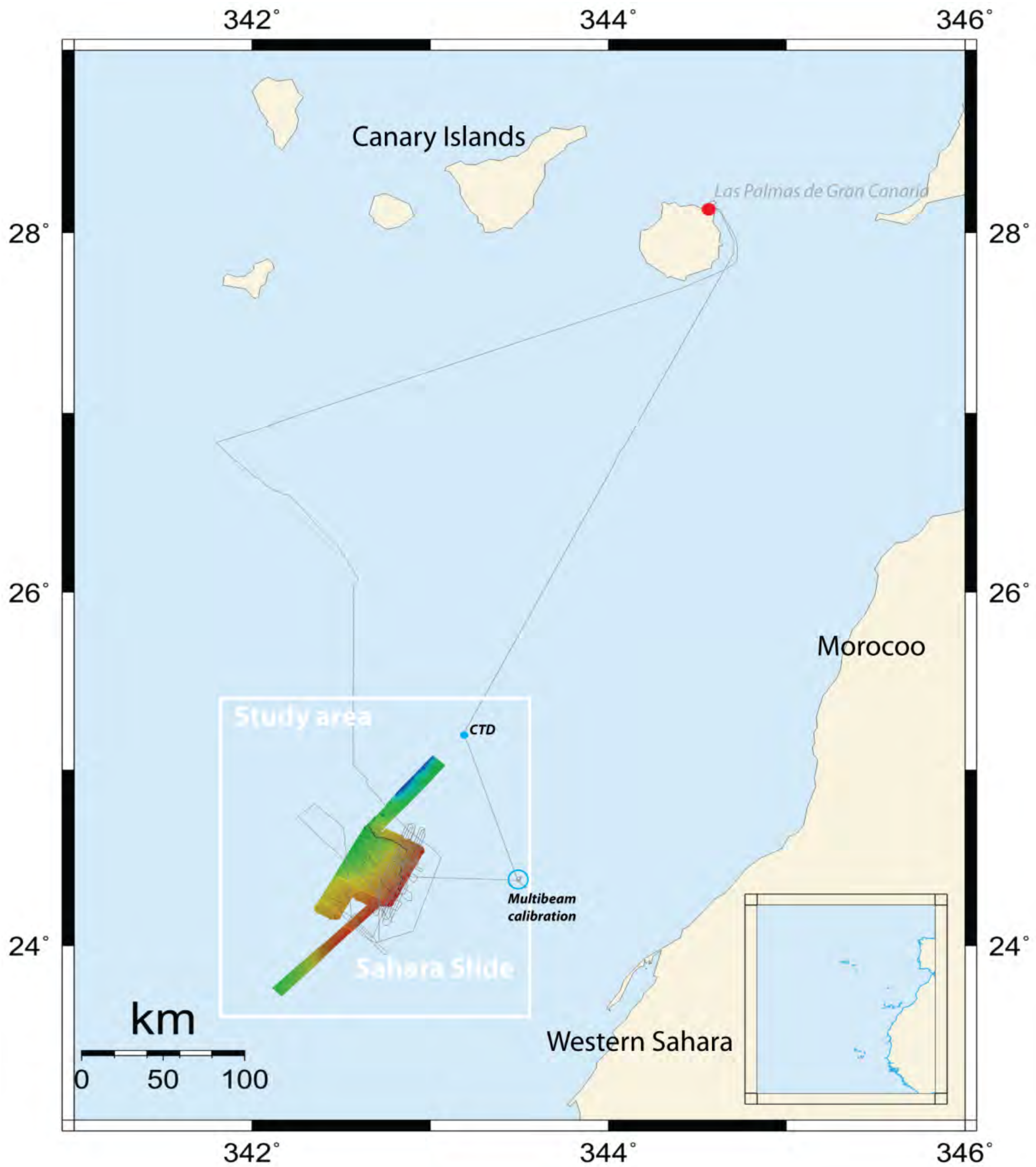

Fig. 6: Cruise track of P395. Location of sound velocity measurement and multibeam calibration are marked by blue circles. Bathymetry data at the Sahara Slide headwall area were collected during Cruise MSM11/2.

4. Narrative of the Cruise

The main group of the scientific party arrived in Las Palmas on February 1st and directly boarded RV Poseidon, which was already in port. The days in port were used to set up the scientific instruments, which was successfully done due to the great support of the crew. We left the port of Las Palmas on February 4th at 09:30h.

The scientific crew of RV Poseidon-Cruise P395 included 6 scientists from the Leibniz-Institute of Marine Sciences (IFM-GEOMAR) and the Cluster of Excellence 'The Future Ocean' (Kiel), one scientist each from Bremen University, National Oceanography Centre Southampton, and University College Dublin, as well as one technician from Oktopus GmbH in Kiel.

After leaving port we headed directly south to a position at 25°11'N, 16°50'W, where we started the scientific program with a CTD run to 2000 m water depth on February 5th at 07:00h. The CTD was needed for collecting a sound velocity profile for the multibeam system. Thereafter we headed to a shelf location around 24°22'N, 16°30'W for calibrating the multibeam system (Fig. 6). Despite the rough sea state, the calibration of the multibeam was successfully finished around 18:00h. The multichannel seismic system consisting of a 200m-long 120 channel streamer and a Mini-GI gun was deployed immediately afterwards. A first seismic profile brought us to the main working area, the headwall area of the Sahara Slide Complex. Two additional profiles crossing the headwall at different locations were collected until February 6th in the morning. A first gravity core (P395-02) in undisturbed sediments above the headwall in ~1900m water depth was taken in the morning of February 6th. The rest of the day was used for calibrating the USBL system for the side scan sonar. Due to some minor problems with the side scan sonar, the night was used for seismic profiling of the head wall area until February 7th in the morning. The seismic data indicate different phases of the main headwall collapse and current influenced sediments in greater sub bottom depth. We started to deploy the side scan sonar together with the multichannel seismic system at 12:00h on February 7th. The side scan sonar is a deep towed EdgeTech 1 system operating at frequencies of 75 kHz and 410 kHz. The first side scan sonar survey was located around the main head wall area. It showed numerous sets of headwalls, tilted blocks, large debris blocks, ridges, and evacuated areas. In total we collected 5 parallel profiles covering an area of 24 x 3.5nm. The system was back on deck on February, 10th at 09:00h. Seismic profiles were collected simultaneously to the side scan sonar. The seismic profile show interesting undulating features with an aggradational wavy pattern covered by a drape.

Based on existing sediment echo sounder data and the new side scan data, 9 core locations were selected close to the headwall along the entire headwall length. Coring was planned for February 10th during day time but due to a high swell, we decided not to start the coring program but running a seismic survey instead. The seismic system was deployed at 10:30h. We collected two long profiles across the lower headwall of the Sahara Slide, which is located in a depth of ~2700m about 30 km seaward of the upper headwall. The seismic data indicate undisturbed strata in vicinity of the lower headwall. No obvious explanations for the location of the lower headwall were identified. In addition we crossed another smaller slide complex south of the main Sahara Slide. The seismic system was retrieved on February 11th at 07:00h. The swell decreased during the night, hence February 11th was used for coring. During the day, we took four cores (P395-03 – P395-06) directly below the southern part of the main slide event. The first two cores showed a debris flow covered only by a very thin drape of undisturbed sediments. The other two cores were located in areas with only very thin or no debrite deposits in order to sample the glide plains at different levels. These old sediments, however, seems to be too stiff for sampling with a gravity corer and recovery was very low. Detailed analyses in the lab will show, if we recovered small pieces of the glide plain sediments. The night was again used for small scale imaging with the seismic system in order to understand the geometry of the underlying sedimentary features. 5 additional cores (P395-07 – P395-11) were taken on February 12th in close vicinity to the northern part of the headwall. Four of the five cores show textbook-like debrites with a very thin undisturbed drape. This observation leads us to the conclusion that the entire upper headwall is a very young feature (~2ka) and not formed during an event about 60ka BP, as postulated before. The fifth core did not recover any sediment as it was located directly on the glide plain, which was again too stiff for sampling. The missing drape on the glide plain, however, supports the idea of a very recent (~2ka) failure.

Coring was followed by mapping with side scan sonar and the seismic systems from the evening of February 12th to February 16th. The mosaic collected during the previous deployment was continued further down slope. The seismic system was not operated along all side scan lines because of currents, waves, and wind resulting in too small lateral distances between the side scan cable and the streamer. In addition the sub-bottom profiler failed during the survey and several lines were collected without the profiler. The survey of the headwall of the Sahara Slide was completed on February 15th in the afternoon. The survey was continued further to the south, where available data showed clear indications for another failure. After crossing the headwall of this failure for the first time on February 16th in the early morning, side scan operations had to be stopped because of a break in the data transmission cable. Due to very high swells we decided to leave the side scan in the water for the rest of the night and recovery of the side scan started at daylight on February 16th. The side scan was on deck at about 09:00h. Unfortunately, the swell was too high for gravity coring. Hence we deployed the seismic system to collect two long slope parallel profiles above and below the headwall.

While collecting the upper slope parallel profile, one of the stabilizers of the vessel failed and we had to change course to a northwesterly direction to head against the swell. Unfortunately it was not possible to repair the stabilizing system at sea. This fact in combination with predicted strong winds led to the decision to stop the scientific program on February 17th at 08:00h. After retrieving the seismic system, we started the transit to Las Palmas. We chose a northerly course at the beginning in order to avoid the swell coming from the side. During the transit the wind increased to force 9-10 with wind peaks up to 62 knots (11-12). From very early morning to the afternoon of February 18th, the vessel was kept stationary due to the strong winds. Decreasing winds and wave heights allowed continuing the transit to Las Palmas in the early evening of February 18th. We reached port on February 19th at 18:00h.

Despite the problems at the end of the cruise and the early stop of the research program, Poseidon Cruise P395 was a great success. We collected more than 800 nm of seismic profiles, mostly in exceptional quality. A large area of the headwall and some areas south of the Sahara

Slide were successfully surveyed with the side scan sonar. In total we collected 10 cores up to 5 m length. Mainly the coring program was affected by the bad weather condition and the early stop of the cruise. Hence coring the lower part of the slide was not possible.

The new data will allow to reconstruct a major slide event from 'source-to-sink' and to assess its geohazard potential.

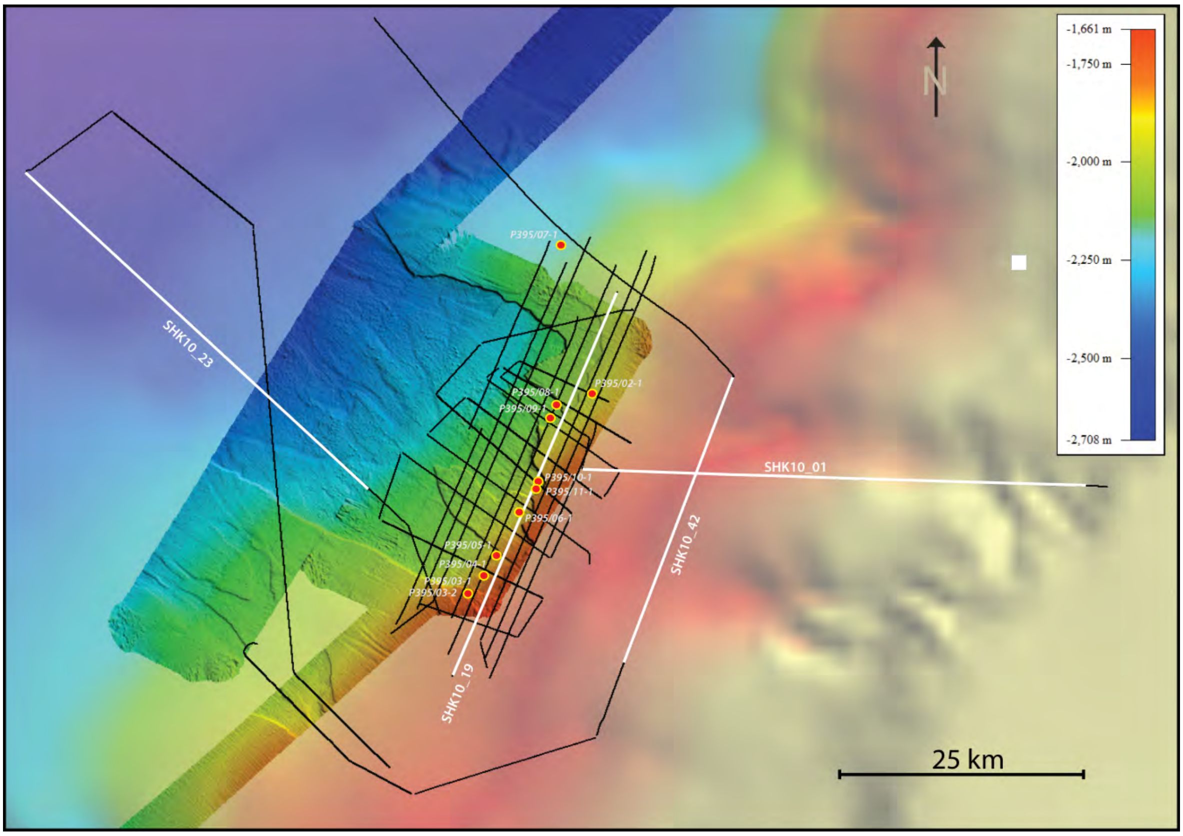

Fig. 7: Headwall area of the Sahara slide with measured seismic and side scan sonar profiles during Cruise P395. White lines indicate positions of seismic profiles shown in Fig. 17 toFig. 20. Locations of gravity cores are marked as red dots. Source of bathymetry data: MSM11/2 and Gebco.

.

5. Preliminary Results

5.1. Bathymetric mapping

Multibeam data from the Sahara Slide headwall area were already collected during Cruise MSM11/2. During Cruise P395 additional multibeam data were recorded to expand the high resolution bathymetry map especially upslope of the headwall area. Therefore a Seabeam 1050 multibeam echosounder system was installed during the cruise which allows high resolution bathymetric mapping.

5.1.1. Technical description

Seabeam 1050 Multibeam Echosounder

The Seabeam 1050 System is a survey system of vast capability and is therefore highly suitable for hydrographic surveys. The operating frequency is 50 kHz. Maximum depth and coverage transverse to the ship is shown in Fig. 8.

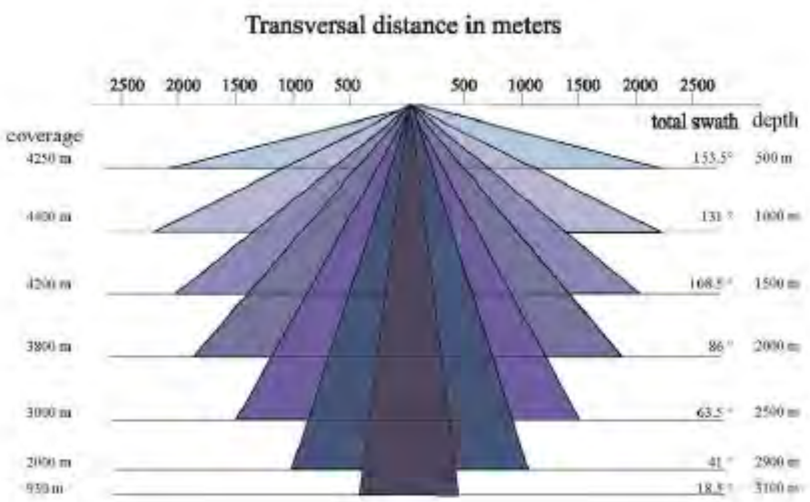

Fig. 8: Maximum depth and coverage of SEABEAM 1050

Two narrow beam width transducer arrays are pinging quasi-simultaneously into 14 directed sectors with a high acoustic transmission level. The receiving beam-former generates 3 narrow beams within each sector with a beam width of 1.5° (Phase calculator) and a spacing of 1.25°. This we call a subfan. A complete fan comprises three subfans, i.e. there are 14 sectors x 3 beams x 3 subfans = 126 beams in total. The relatively high operating frequency of 50 kHz in conjunction with special small size transducers offers two advantages: high coverage and narrow beam width. The application of preformed beams guarantees extremely good side lobe suppression and a very low error rate. This has a positive influence on measuring accuracy and gives the system a big advantage over one way procedures, i.e. non-directed transmission and reception.

Transducer arrays LSE 237

The SEABEAM1050 system employs two transducer arrays of type LSE 237, port and starboard, both capable of transmitting and receiving. Their acoustic planes are tilted 30° to the horizontal. The arrays are normally installed fixed to the ship's hull. Onboard of RV Poseidon the two transducers are deployed at the hull of the vessel through the "moon pool". Position of the transducers can be seen on Fig. 9.

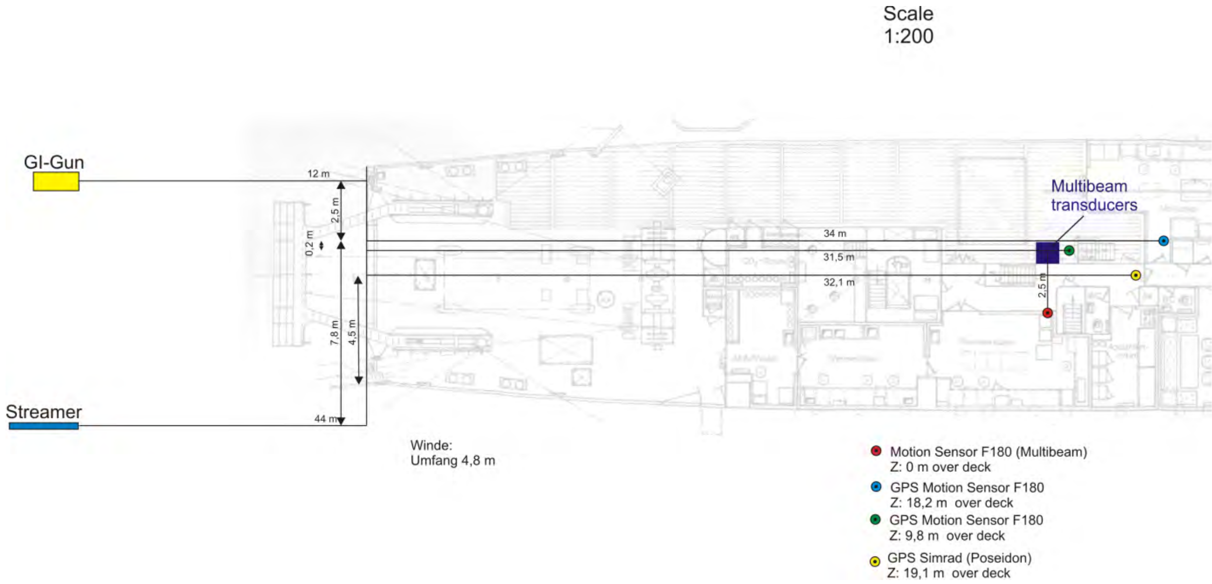

Fig. 9: Deck setting with GPS positions during P395 cruise.

The ultrasonic transducer LSE 237 is used to transmit and receive ultrasonic impulses at a frequency of 50 kHz. It consists of 32 separate staves. By triggering the separate transducer staves with a phased transmit signal it is possible to point the direction of transmission to ± 50° with respect to the normal „untreated" array transmission angle. In the transmit path both transducer arrays operate in parallel with a common power stage. All 32 staves of each transducer array are used for transmit beamforming. In the receive path port and starboard array signals are handled separately. 16 center staves of each transducer are used to form narrow beams. The number of beams and fan width is selectable.

Control Unit SEE 30

The Transmit/Receive Unit SEE 30 is accommodated within a transportable case (Fig. 10). It consists of a number of plug-in components contained in a rack.

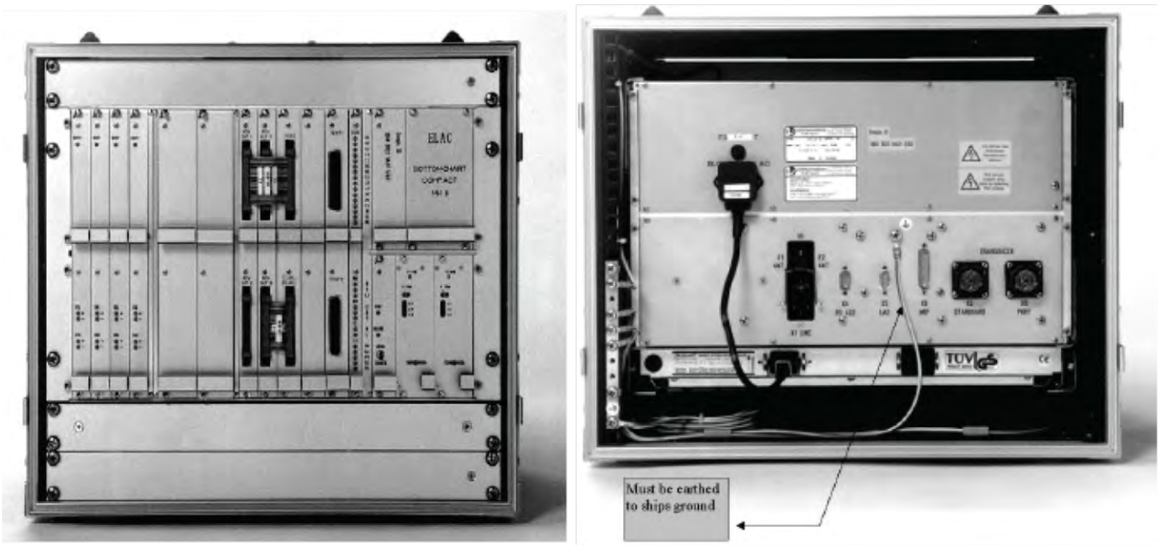

Fig. 10: Front and rear view of the control unit SEE 30.

Motion Sensor Octopus F180

The motion sensor Octopus F180 provides roll compensation signals to the system as well as pitch and heave correction signals to the processor. In addition, it also provides heading information to the data acquisition system. For motion correction of the multibeam measurement the motion sensor should be installed close to the transducers. Position of the F180 motion sensor can be seen on Fig. 9.

GPS-Receiver GARMIN 152

A GPS-receiver GARMIN 152 was used to get information on exact positions. The position data was provided to the data acquisition system in NMEA protocol via a serial interface.

Data acquisition

Data acquisition station was a standard industry size 19" PC, operating system was Windows XP professional. Operator interface includes a 19" graphic monitor, keyboard and mouse. To enable input of several sensor data via serial lines a special 8-port serial interface was installed. For data acquisition L3 communications ELAC Nautik online software Hydrostar 3.5.3 was used.

Sound velocity measurements

For correct measurement of multibeam data a water sound velocity profile is needed and was recorded on February 5th before multibeam calibration was done. Position of the sound velocity profile was 25°11'N, 16°50'W with a depth of 2000 m (Fig. 6, Fig. 11). A CTD probe measures conductivity, temperature and salinity while lowering on a wire. From the continuous recording of these values a velocity profile can be calculated representing the sound velocity distribution in the water column.

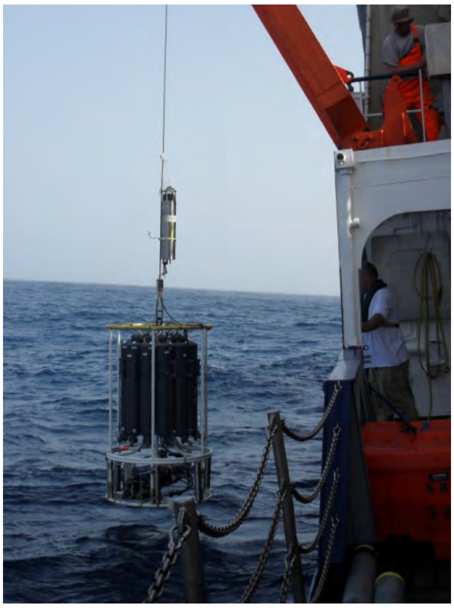

Fig. 11: Lowering of the CTD for sound velocity measurement.

After the sound velocity profile was taken, roll calibration of the multibeam system was run to determine the bias of the system with respect to the horizontal. Therefore a small profile on relatively plain sea floor topography is measured in both directions. Difference in the inclination across track of both multibeam recordings can be calculated. The Seabeam system uses this information for correcting the measured multibeam data.

Multibeam calibration was not carried out perfectly. Hence the quality of the recorded multibeam data is rather low. Significant amount of noise in combination with water depths close to the limit of the system (~2000 m) resulted in very poor data quality.

5.1.2. Results from bathymetric mapping

Fig. 12 shows a map of the recorded multibeam data from cruise P395. Filter mechanisms have already been applied to the data but did not improve the data quality significantly. The continental slope is imaged at a depth range from about 1000 m ca. 2500 m. However, as mentioned above, a poor calibration in combination with other factors resulted in very poor data quality.

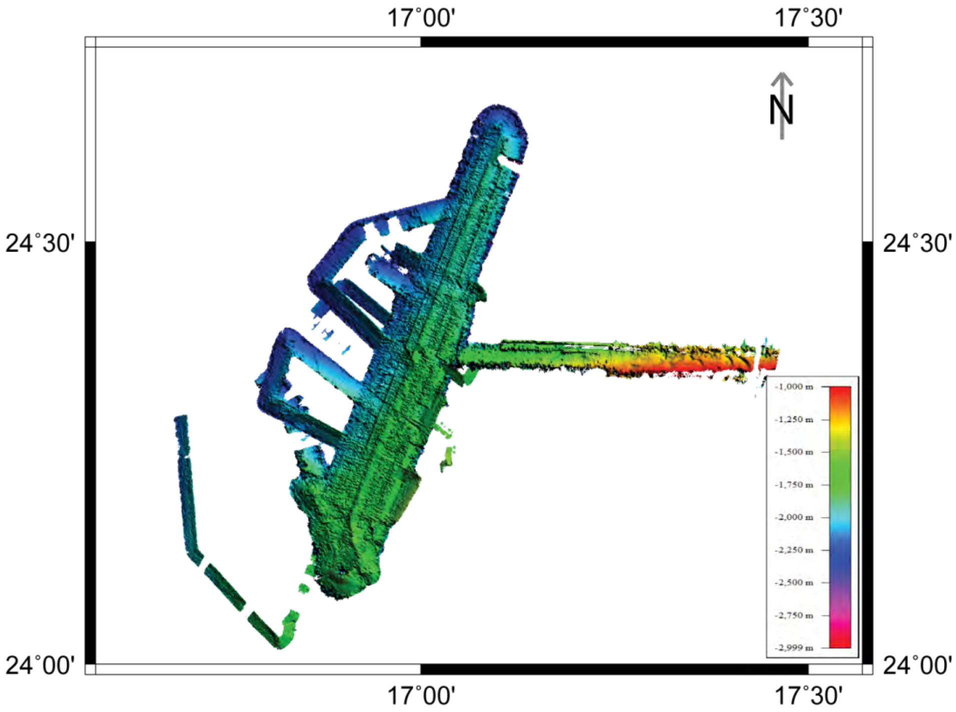

Fig. 12: Bathymetric map of the recorded multibeam data during P395 cruise.

5.2. High resolution multichannel seismic profiling

A high resolution multichannel seismic survey was carried out during P395 with the aim to resolve sedimentary structures along the continental margin. A micro GI gun was used as a source for transmitting signals. A 200 m-long 120-channel digital streamer was used for recording the reflected energy down to 1s TWT subsurface depth.

Seismic source

During Cruise P395 a micro GI gun (Fig. 13) was used as a seismic source. The gun was shot in harmonic mode with a volume of 2 x 0.1l; the main frequency is ~200 Hz. The Injector was triggered with a delay of 20 ms after the Generator for depressing the bubble signal in the recorded seismic data. The Micro-GI Gun was towed about 1 m below the water surface. Shooting rate was adjusted to the water depth, varying between 5.5 and 7 seconds resulting in a shot point distance of 7 – 14 m at 2.5 - 4 knots. The gun was shot at an air pressure of around 150 bars provided by two mobile diving compressors.

Fig. 13: Micro GI-Gun used during seismic surveying on P395.

Streamer system

A digital streamer (Geometrics GeoEel) was used for receiving the seismic signals (Fig. 14). The system consists of a tow cable (80 m, 33 m in the water), one stretch section (25 m) and 15 active sections (each 12.5 m). An active section contains 8 channels (channel spacing of 1.56 m) resulting in 120 channels within the total streamer (Fig. 15). One AD digitizer module belongs to each active section. These AD digitizer module are small Linux computers. Communication between the AD digitizer modules and the recording system in the lab is via TCP/IP. A repeater was located between the deck cable and the tow cable (Lead-In). The SPSU manages the power supply and communication between the recording system and the AD digitizer modules. The recording system is described below. Three birds were attached to the streamer (see below). Designated streamer depth was 3 m. A small buoy was attached to the tail swivel. From profile 035 on the last active section of the streamer was removed because of leakage problems and only 14 sections (112 channels) were used.

Fig. 14: Picture of the streamer system (on the winch) used during Cruise P395.

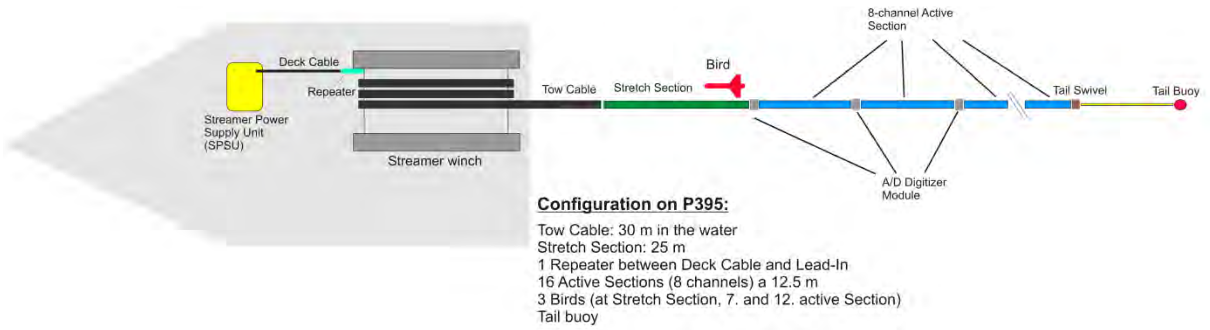

Fig. 15: Streamer configuration during Cruise P395.

Bird Controller

Three Oyo Geospace Bird Remote Units (RUs, Fig. 16) were deployed at the streamer. The positions of the birds are listed in Table 1. All RUs have adjustable wings. The RUs are controlled by a bird controller in the lab. Controller and RUs communicate via communication coils nested within the streamer. A twisted pair wire within the deck cable connects controller and coils. Operating depth of the birds was set to 3 m. Due to rough weather conditions depth of the birds varied strongly especially during the last part of the cruise.

	Distance behind stern			
Profile	**Bird 20376**	**Bird 20398**	**Bird 20399**	**Bird 20415**
001-005	--	58	145	208
006-014	145	58	--	208
015-034	58	145	--	208
035-043	58	145	--	208

Table 1: Birds Position during P395

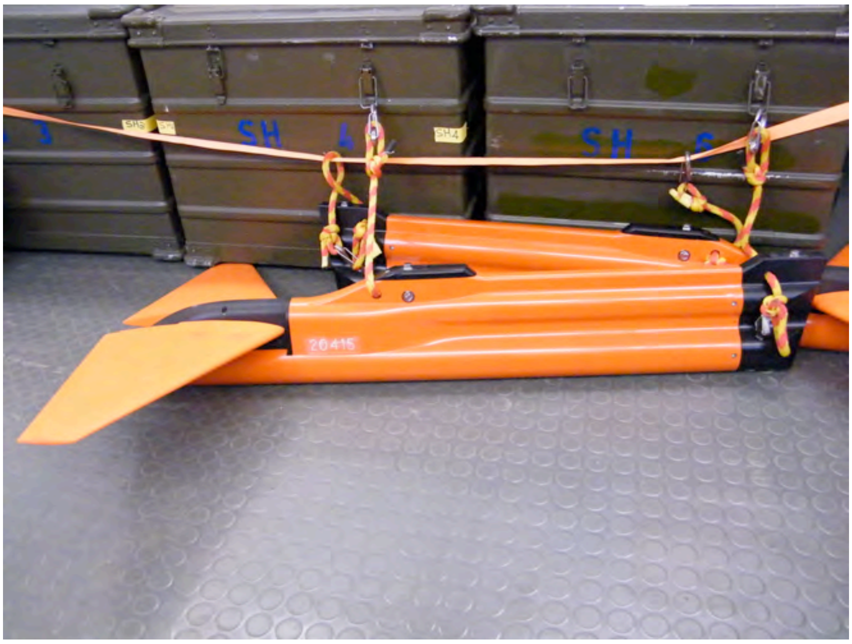

Fig. 16: Birds fixed on deck, before attaching to the streamer.

Data acquisition systems

Data of the streamer were recorded with acquisition software provided by Geometrics. The data were recorded at 4 kHz as multiplexed SEG-D. One file was generated per shot. Data were recorded with delay but the delay is not written to the header. The delay was adjusted to the water depth. Recorded time length of each SEG-D file was set to 3 seconds. The acquisition laptop allowed online quality control by displaying shot gathers, a noise window, and the frequency spectrum of each shot. The cycle time of the shots is displayed as well. The software also allows online NMO-correction and stacking of data for displaying stacked sections. Several log files list parameters such as shot time and shot position. Data were converted to SEG-Y file while being at sea.

Trigger unit

A custom trigger unit, the so called SchwaBox was used during the cruise. The box generates triggers (TTL) at arbitrary combinations for controlling seismic sources, acquisitions systems, and bird controllers. The box was also connected to a gun amplifier unit. The trigger scheme was adjusted to the water depth during the survey. This trigger system worked very reliable during the entire cruise.

Results from seismic surveying

Onboard processing of the seismic data has been performed including band-pass-filtering, applying static shift, and stacking of several channels in order to create so called brute-stacks.

The slope parallel profile SHK10_01 (Fig. 17) shows part of the continental margin upslope of the Sahara Slide headwall area pointing out some characteristic features of the study area. The steep slope at the eastern end of the profile images various parallel to subparallel reflectors. The main dip direction of these sediments is towards the west although the dip angle is varying. At around 300 m water depth a plateau is visible. Seismic data suggests significant erosion along the steep continental slope. Incisions within the uppermost sediment layers might be due to channel systems. The seismic data allows defining three seismic units (A-C) from offset 40000 m towards the west. The deepest unit (A) is characterized by reflectors of rather low amplitudes dipping to the west. Signal attenuation is too strong for resolving the deeper parts of this unit. The boundary towards Unit B is imaged as a strong slope parallel reflector overlain by rather diffuse reflections of low amplitudes which are getting stronger and more chaotic towards the top of Unit B. The lower boundary of the youngest Unit C is characterized by a zone of extremely low amplitude reflectors. The wavy pattern of this zone is present also in the overlying higher amplitude reflectors most likely representing sediment waves especially in the central part of the profile where they can be traced up to the sea floor. Sediment waves in the western part of the profile are buried beneath slope parallel, westward dipping reflectors.

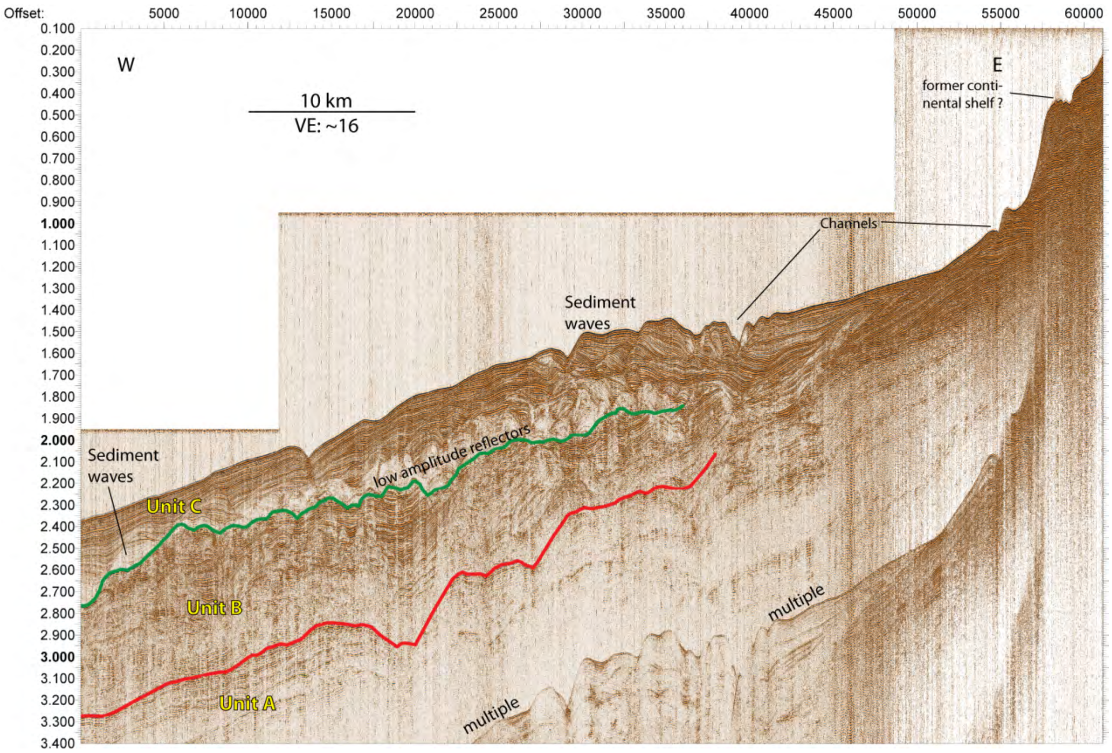

Fig. 17: Brute stack of seismic profile (SHK10_01) running from the shelf edge to the headwall area of the Sahara Slide Complex. See Fig. 7 for location of profile.

Fig. 18 shows a profile (SHK10_19) running slope parallel and crossing the two sidewalls of the Sahara Slide. The three seismic units (A-C) are visible although transition between Unit A and Unit B is difficult to detect. Unit A and the deeper part of Unit B are characterized by low amplitudes. Unit B includes three SE-NW striking mounds characterized by high amplitude reflectors of moderate continuity. Deep seismic data do not show any salt diapirs in this area. We speculate that these mounds were formed by ocean currents though the height of these mounds is significantly higher than those of other known mounds formed by currents. A clear incision is visible at the crest of the central mound. The troughs between the mounds are filled by younger sediments of Unit C imaged as low amplitude reflectors (thickness of 0.3 -0.4 sec TWT). Well stratified layers of moderate amplitude with a slightly wavy pattern are found on top of the low amplitude reflectors and the mound-like features. Within Unit C wavy sediments can be observed in the southern part of the profile and on top of the central sediment mound. The uppermost layers of Unit C are relatively undisturbed while the sea floor itself clearly shows several features of the scar area including the steep headwall, sidewalls, and rough sea floor morphology in the central part of the slide (Fig. 18). It is evident that the outer two sediment mounds are aligned with the sidewalls while the central mound coincides with the position a westward overhanging part of the headwall.

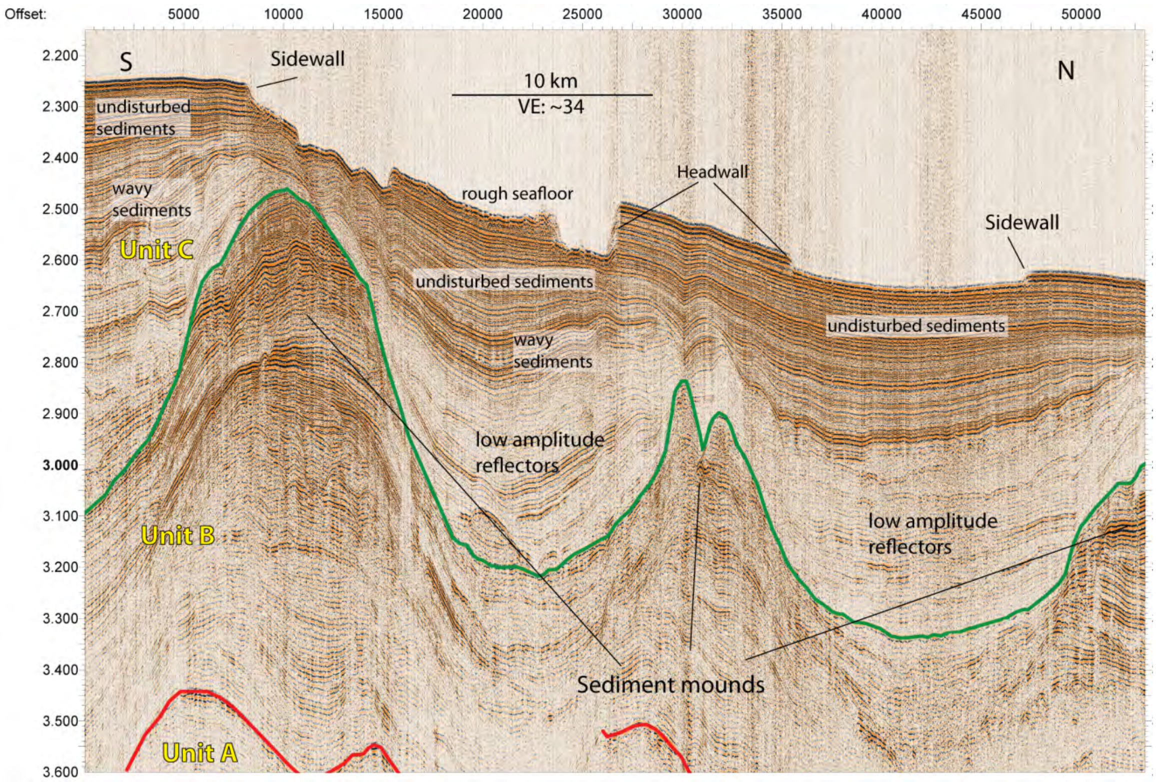

Fig. 18: S-N running seismic profile (SHK10_19) with seismic Units (A-C) including sediment mounds, low amplitude reflectors, and undisturbed sediments. Features of the scar area include headwalls, sidewalls, and a rough sea floor morphology. See Fig. 7 for location of profile.

The sediment mounds are also found on Profile SHK10_42 (Fig. 19) upslope of the Sahara Slide headwall but with smaller dimensions. The mounds visible on Fig. 19 correspond to the southern and central mound of Fig. 18. A small incision is visible at the crest of the central mound. Seismic Units B and C are separated by low amplitude reflections at the base of Unit C. The strong reflectors on top show a slightly wavy pattern, while undisturbed sediment layers can be traced up to the sea floor. Two troughs roughly located above the lows of the mounds are found at the sea floor. The sea floor itself appears relatively smooth. At the northern part of the profile a bottom simulation reflector (BSR) is visible at a depth of 0.3 sec TWT below the surface pointing to the presence of gas hydrates.

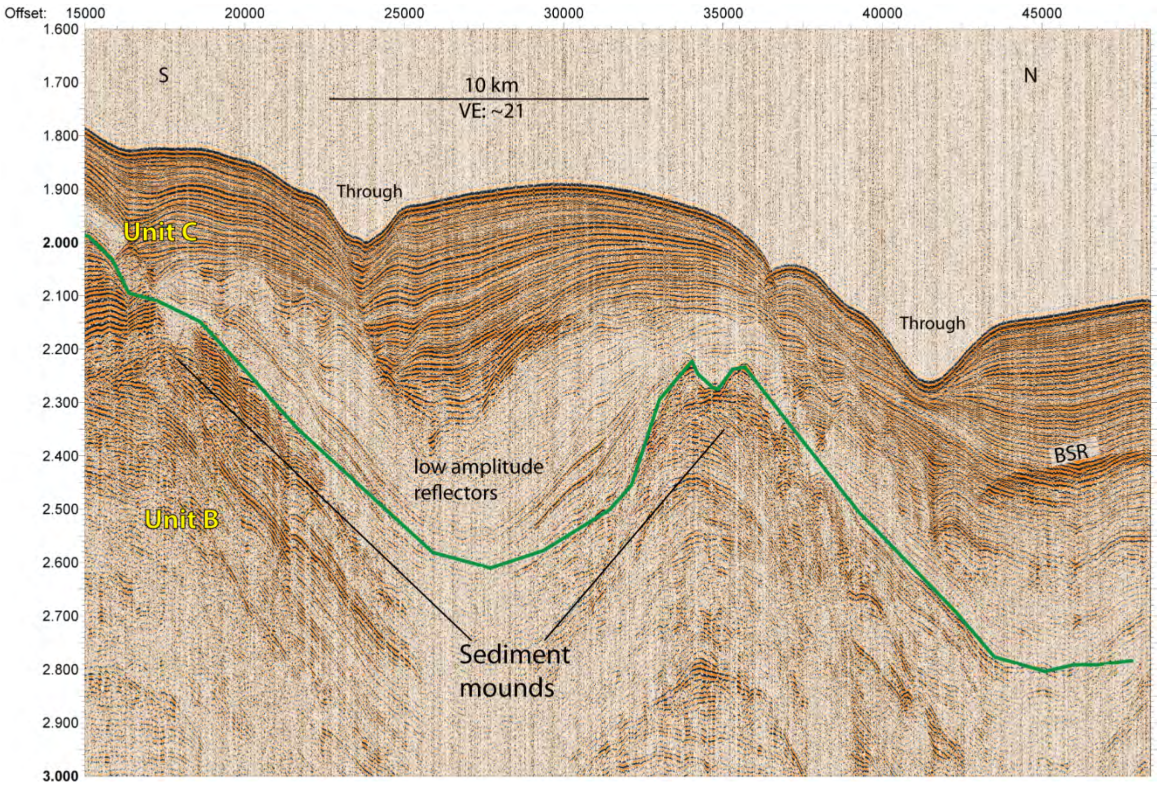

Fig. 19: Brute stack of seismic profile SHK10_42 upslope of the Sahara Slide headwall. A Bottom simulating reflector (BSR) appears at the northern part of the profile. See Fig 7 for location of profile.

The lower headwall of the Sahara Slide is imaged on Profile SHK10_23 (Fig. 20). Data quality is relatively poor due to bad weather conditions and the large water depth, but only less than 10 percent of all available traces are used for this brute stack. Hence fully processed image will result in significantly better imaging quality. Only seismic Units B and C are visible separated by a strong slope parallel reflector. The upper part of Unit B shows some diffuse high amplitude reflections while beneath the uppermost 0.1 sec TWT of Unit B individual weak reflectors image westward dipping layers. Unit C is characterized by several zones of low amplitudes (thickness between 0.05 and 0.1 sec TWT) separated by a strong slope parallel reflector. This alternation continues close to the surface. Within the uppermost layers of the southeastern part of the profile no low amplitude zones are visible. The sea floor is relatively rough along the whole profile with two prominent morphological steps: the lower step represent the main location of the lower headwall. It is about 100 m high. Slide deposits beneath this headwall are imaged as transparent-to-chaotic sediment body. The slide material is deposited above a strong slope parallel reflector, probably a glide plane for the sliding sediments (Fig. 20, blue line). Another clear step at the northwestern part marks an internal slide scarp. Slide deposits characterized by chaotic low amplitude facies can be found down slope of this headwall scarp deposited on a potential glide plane imaged as high amplitude reflector.

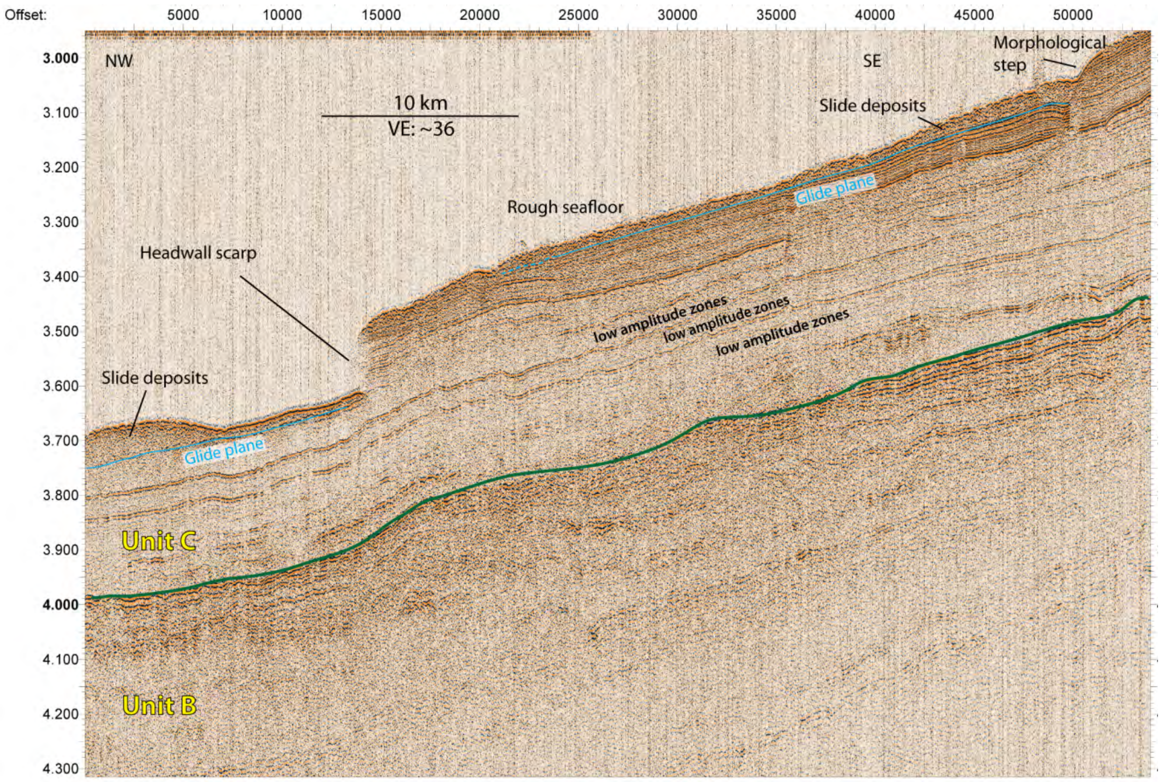

Fig. 20: Brute stack of Profile SHK10_23 crossing the lower headwall of the Sahara Slide Complex See Fig. 7 for location of profile.

5.3. Side scan sonar mapping

A side scan sonar was deployed during Cruise P395 in order to investigate sea floor morphology and sedimentary features along the landslide area and to detect changes in surface material. The side scan sonar system includes a towfish with transducers, a recording device on board, and a tow cable.

The transducers are composed of a series of piezoelectric elements and mounted to the sides of the towfish. The signal transmitted by the transducers is attenuated with distance, which means that the intensity of the emitted signal decreases with increasing distance, which is called spherical divergence. The degree of attenuation is dependent on the frequency of the acoustic signal (Mitchell, 1993). The propagation of acoustic signals is also affected by noise and objects in the water column. Most of the energy reaching the sea floor is reflected. As long as the sea floor does not act as a perfect mirror scattering of the acoustic signal occurs at the sea floor. Part of the scattered signal is directed back to the sonar's receivers where this backscatter signal is amplified and recorded over time (Fig. 21).

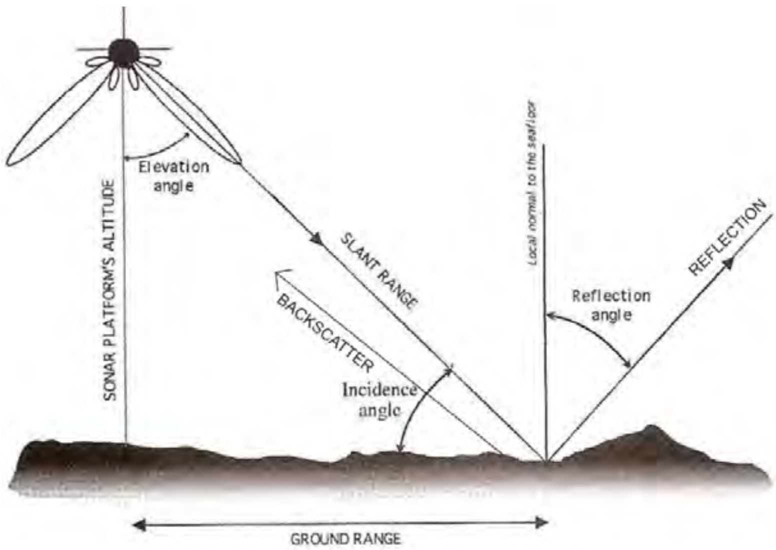

Fig. 21: Scheme of sonar data acquisition. Slant-range is the distance travelled from the transducers to the sea floor. The horizontal distance between nadir of the sonar and the target is called ground range. Acoustic signals are transmitted from the sonar's transducers to the sea floor. A small amount of the energy is scattered back to the sonar and recorded over time (Blondel & Murton, 1997).

Frequencies used by side scan sonar systems in combination with height of the fish above the sea floor, ping repetition rate, pulse length, and swath width control the pixel size of the ensonified areas and thus the quality of the resulting sonar image (Johnson & Helferty, 1990). The backscatter level is the most important information from sonar images characterizing the roughness of the sea floor (Blondel & Murton, 1997). The backscattering strength is defined as the ratio of the backscattered (spherical wave) to the incident wave (plane) intensity. Backscattering from the sea floor is influenced by three factors (Blondel & Murton, 1997):

- ➔ Local geometry of the sensor-target system (e.g. angle of incidence, local slope)
- ➔ Physical characteristics of the sea floor (e.g. roughness)
- ➔ Intrinsic nature of the surface (e.g. density, composition, rocks vs. sediments)

Backscatter values derived from side scan sonar measurements therefore provide information about sea floor morphology and surface material and can be used to analyze sedimentary processes at the sea floor (Fig. 22). For Cruise P395 an EdgeTech DTS-1 side scan sonar was used with an integrated sub-bottom profiler, which provides information about the subsurface structure.

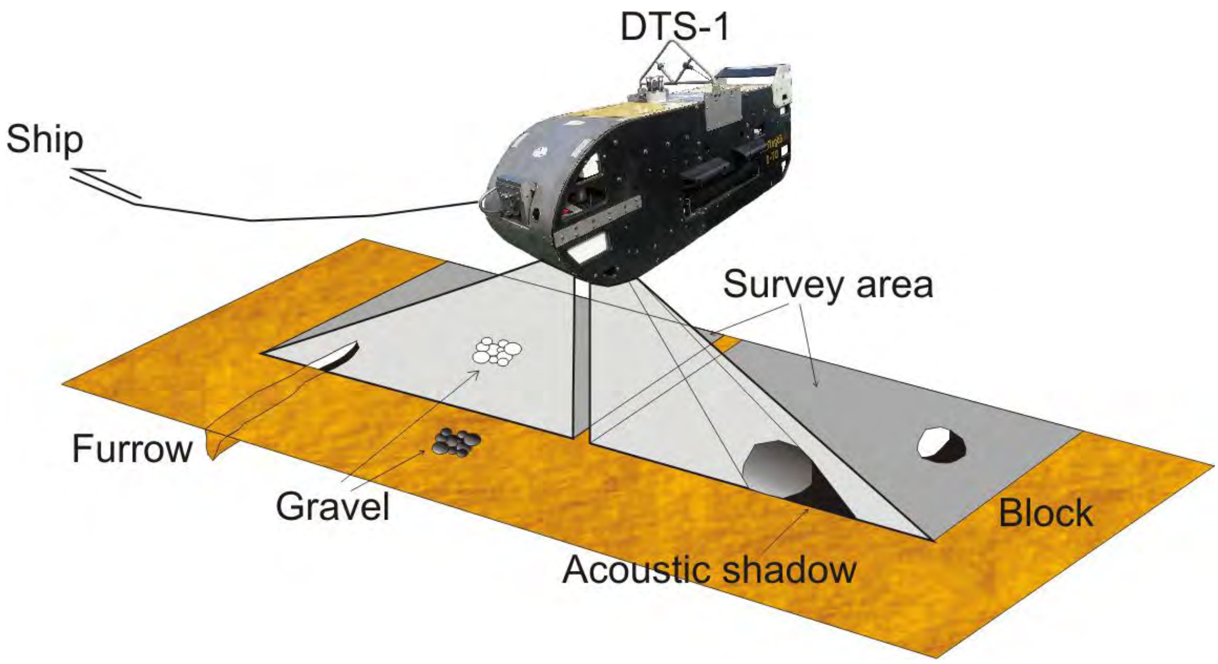

Fig. 22: Scheme of sonar deployment and received signal of the survey area. High backscatter is marked by white, low backscatter by black colors. Big blocks, boulders, and gravel yield high intensity backscatter from the side facing the sonar accompanied by low backscatter on the other side due to a shadow zone of the acoustic signal. Negative features like furrows have shadows on the side closer to the sonar which cannot be ensonified by the acoustic signal. With decreasing grain size intensity of backscatter is also decreasing.

5.3.1. DTS-1 Side scan sonar system

The DTS-1 is based on an EdgeTech dual-frequency chirp system which means that the signal frequency changes with time. The two operating frequencies are centered at 75 kHz and 410 kHz providing a range per side of 750 and 150 m, respectively (Klaucke et al., 2010). The 75 kHz signal is a 14 ms long pulse of 7.5 kHz bandwidth while the 410 kHz signal has a bandwidth of 40 kHz with a 2.4 ms long pulse. These frequencies yield across-track resolutions of 5.6 cm and 1.8 cm, respectively. Along-track resolution is dependent on the survey speed which is ideally around 2.5 knots (Klaucke et al., 2006; 2010). For this study only the 75 kHz signal was used; swath width was 1500 m.

The raw data were processed for a pixel size of 1 m. During Cruise P395 the fish was towed behind the vessel around 100 m above the sea floor, acoustic signals were transmitted every 1.023 sec. Unfortunately the USBL system did not work during the cruise and the layback of the towfish was computed from the length of cable out and simple trigonometric relations assuming the cable is straight. This procedure was complicated by failures of the cable length indicator. Nevertheless, a reliable position of the towfish could be reconstructed, and the resulting sonogram mostly matches with the features observed in the bathymetry. Further navigation processing will be carried out at a later stage.

5.3.2. Sub-bottom profiler

The sub-bottom profiler (SBP) deployed during Cruise P395 is integrated in the side scan sonar system DTS-1 operating with chirp based frequencies between 2 kHz and 10 kHz and 20 ms pulse length. These frequencies provide a penetration depth of up to 30 m (dependant on sediments) and a vertical resolution of a few decimeters (Klaucke et al., 2010). The SBP worked very reliable for most of the time. A cable break during the last deployment resulted in missing SBP-coverage for a few sonar lines.

5.3.3. First Results

After processing the side scan sonar mosaic provides a detailed acoustic image of the sea floor in the headwall area of the Sahara Slide with a lateral resolution of 1 m (Fig. 23). Various features and facies can be identified due to variations in backscatter.

In the north and south two major headwalls are visible both belonging to the upper headwall complex of the Sahara Slide. The undisturbed deposits outside of the slide scar are fine-grained hemipelagic slope sediments. These deposits occur as homogenous low backscatter areas in the side scan sonar data. Different sized debris and blocks are present within the slide area. The central area is dominated by rails and large individual blocks. At least two big lobes, enclosing the central area (named lobe and tongue on Fig. 23) as well as two additional smaller lobes in the south are visible in the scar area.

The area beneath the northern part of the headwall (blocky area north on Fig. 23) shows numerous elongated blocks clearly contrasting the undisturbed sediments outside the slide area. These blocks have lengths of up to 600 m (Fig. 24) and are exclusively orientated slope parallel with slightly wavy pattern independent from their size. The sea floor outside of the slide area as well as the region below the lower headwall shows low and more homogenous backscatter values indicating a smooth surface without major blocks.

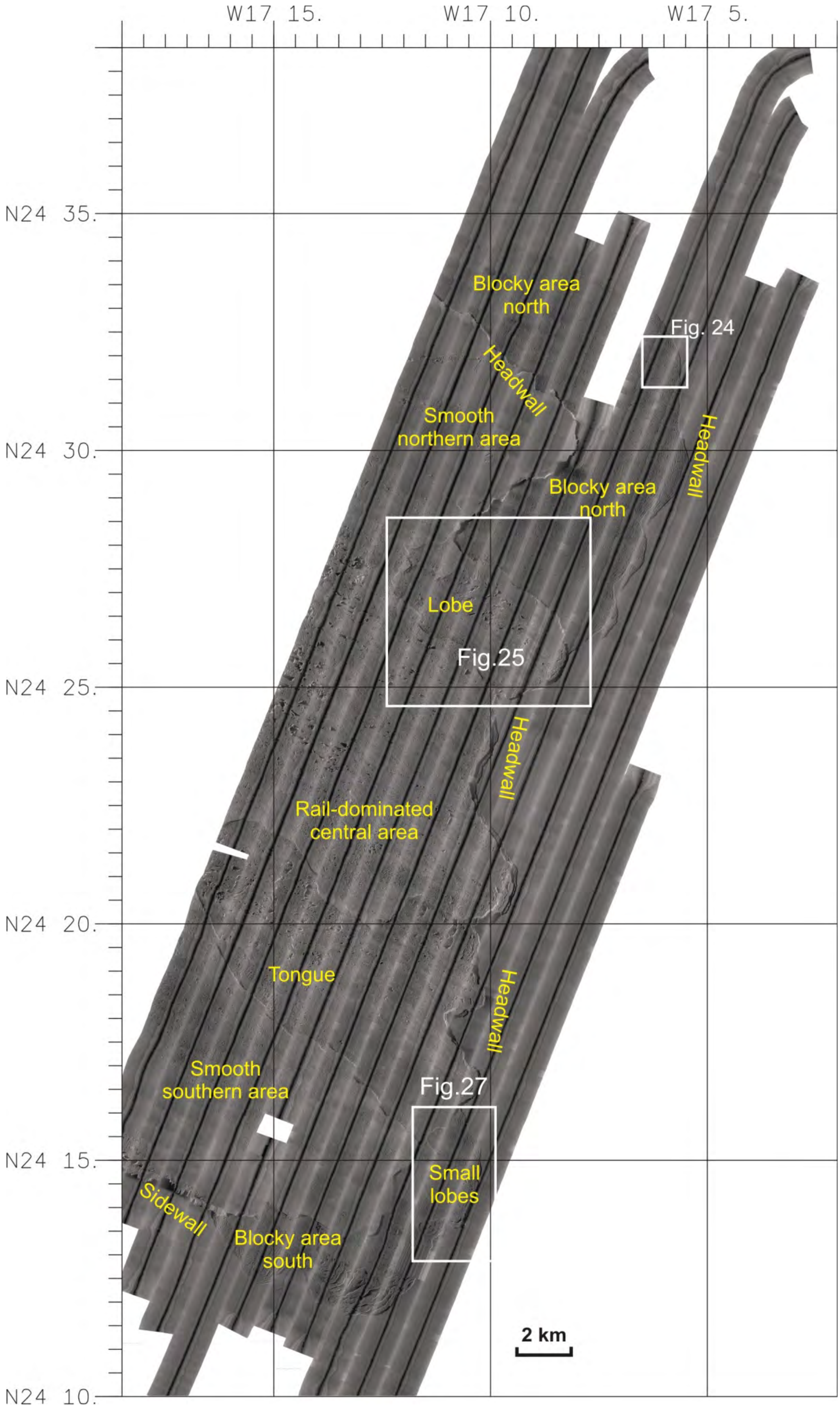

Fig. 23: Side scan sonar mosaic of Cruise P395 showing the headwall area of the Sahara Slide. Dark colors represent areas of low backscatter.

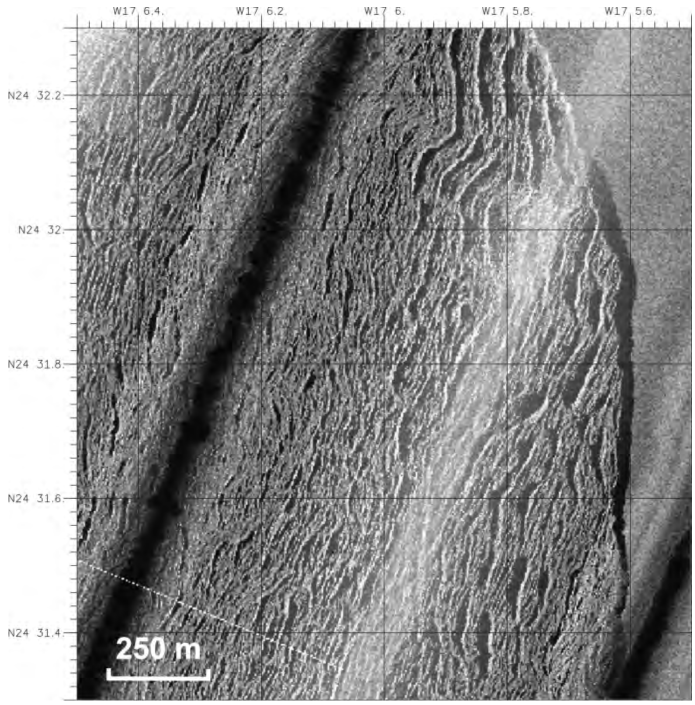

Fig. 24: Eastern part of the 'blocky area north' showing the upper headwall and elongated blocks just below the headwall. Location of sonogram is marked on Fig. 23.

Further south a lobe of approximately 7.5 km length and 3.7 km width is bordering the blocky area (Fig. 25). The headwall separating the lobe and the 'blocky area north' is defined by the blue dashed line and has a height of about 35 m while the height difference between the lobe and the central area to the south is approximately 30 m. The central part of the lobe is characterized by a zone of large blocks of up to 230 m length. This blocky area is surrounded by smooth surfaces with low backscatter values showing a down slope orientation, so called rails. Major blocks are found at the edges of most major rails. A sub-bottom profile image (Fig. 26) crossing the western part of the lobe shows a rough surface with low penetration into deeper sediments. Two prominent reflectors are visible at the south-western edge of the lobe. One internal step is visible in the lobe area. The step to the central slide area in the south has a slope gradient of ~12° and a step height of ~27 m. Rails are imaged as smooth areas being free of major slide deposits(Fig. 26).

Within the southern part of Sahara Slide the upper headwall clearly separates undisturbed slope sediments from the slide area (Fig. 27). Two small lobes of approximately 1 km and 2.5 km length are found in the southern part of the Sahara Slide headwall area (Fig. 27). They are imaged directly below the headwall. Their surface is characterized by big blocks which are orientated along-slope. A cross section of the two lobes can be seen in the SBP data of Fig. 28 showing rails between the lobes and few parallel and diffuse subsurface reflectors.

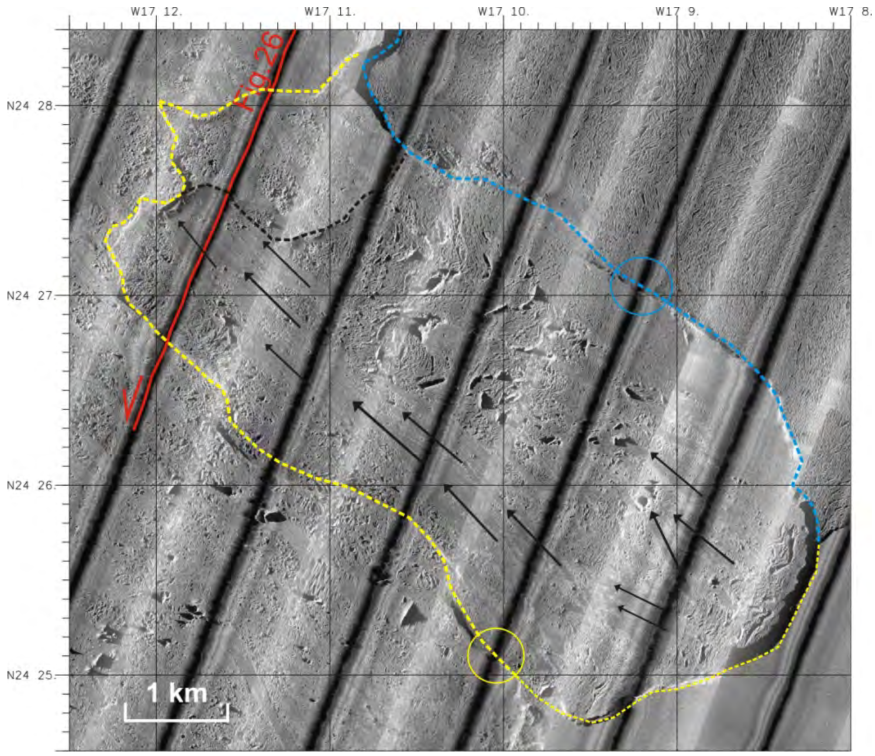

Fig. 25: The outline of the lobe is marked by the dashed yellow and blue lines. The blue line marks the boundary to the 'blocky area north' while the yellow line marks the step to the central slide area. Some rails are marked by black arrows. The SBP line of Fig. 26 crossing the western edge of the lobe is marked as red line.

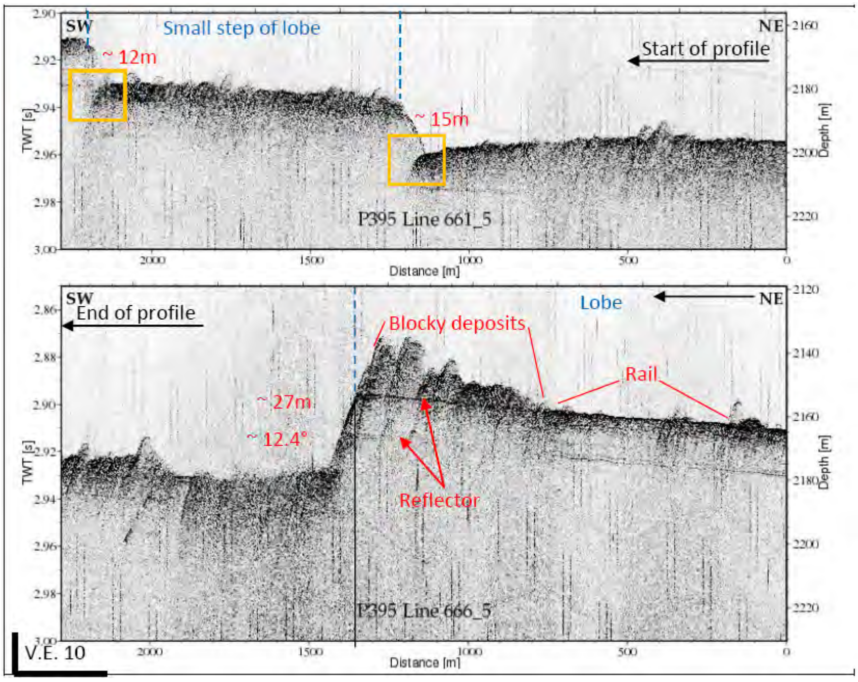

Fig. 26: SBP image crossing the distal part of the lobe (boundaries of lobe are marked by the blue dashed lines). Blocky deposits are characterized by hyperbolas. Rails show an almost smooth surface. The yellow boxes mark overlapping surfaces, which are caused by edge effects during data acquisition. See Fig. 25 for location of profile.

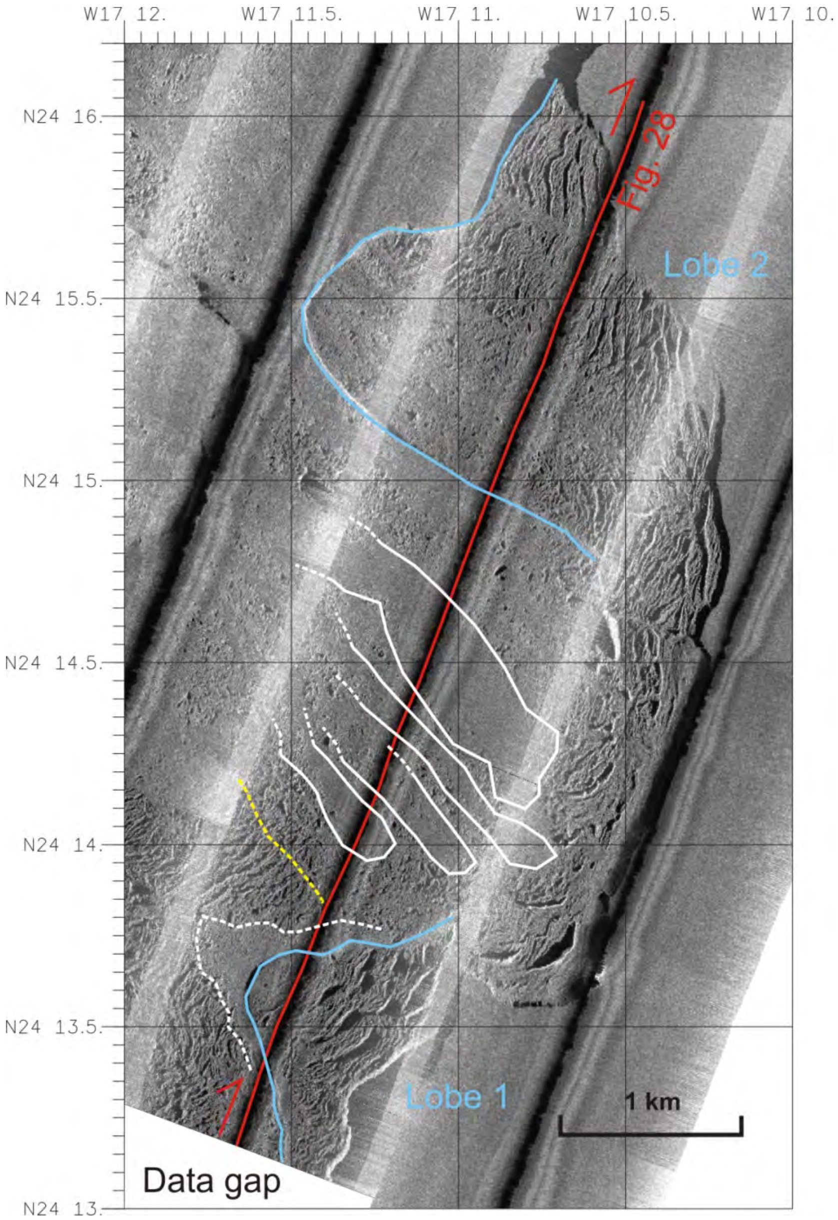

Fig. 27: Sonogram showing two small lobes in the southern part of the Sahara Slide headwall area (blue lines). The surface of the lobes is characterized by large orientated blocks. The surface is covered by small-sized debris and dissected by rails (white lines) between the lobes. See Fig. 23 for location of sonogram.

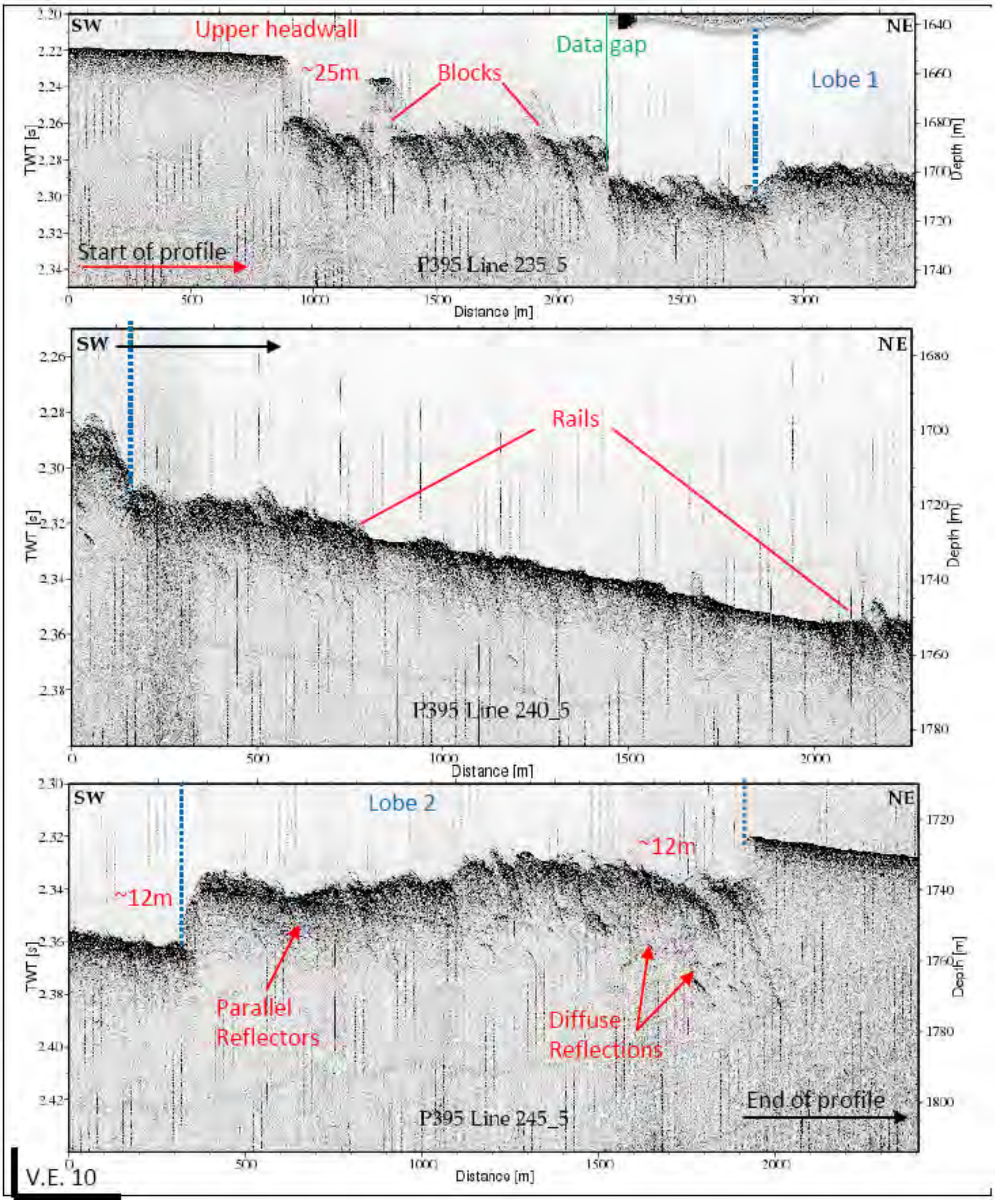

Fig. 28: SBP data crossing two small lobes. Both lobes are separated from the surrounding features due to elevated topography. The area is characterized by blocky deposits and rails between the two small lobes. See Fig. 27 for location of profile.

5.4. Sediment Sampling

The sedimentological sampling program focused on the main sedimentary structures of the Sahara Slide area and on recovery of gravity cores for dating of failure events.

Ages of distal deposits from the Sahara Slide indicate failure 60.000 years ago (Embley, 1982; Gee et al., 1999; Georgiopoulou et al., 2007). Recent studies indicate Holocene slope failure events as young as app. 2.000 years (Geogiopoulou et al., 2009). Therefore, the sampling strategy concentrated on the recovery of cores from the upper headwall to gain additional information on recent failures. We term this first target area for sampling Area 1 (Fig. 29).

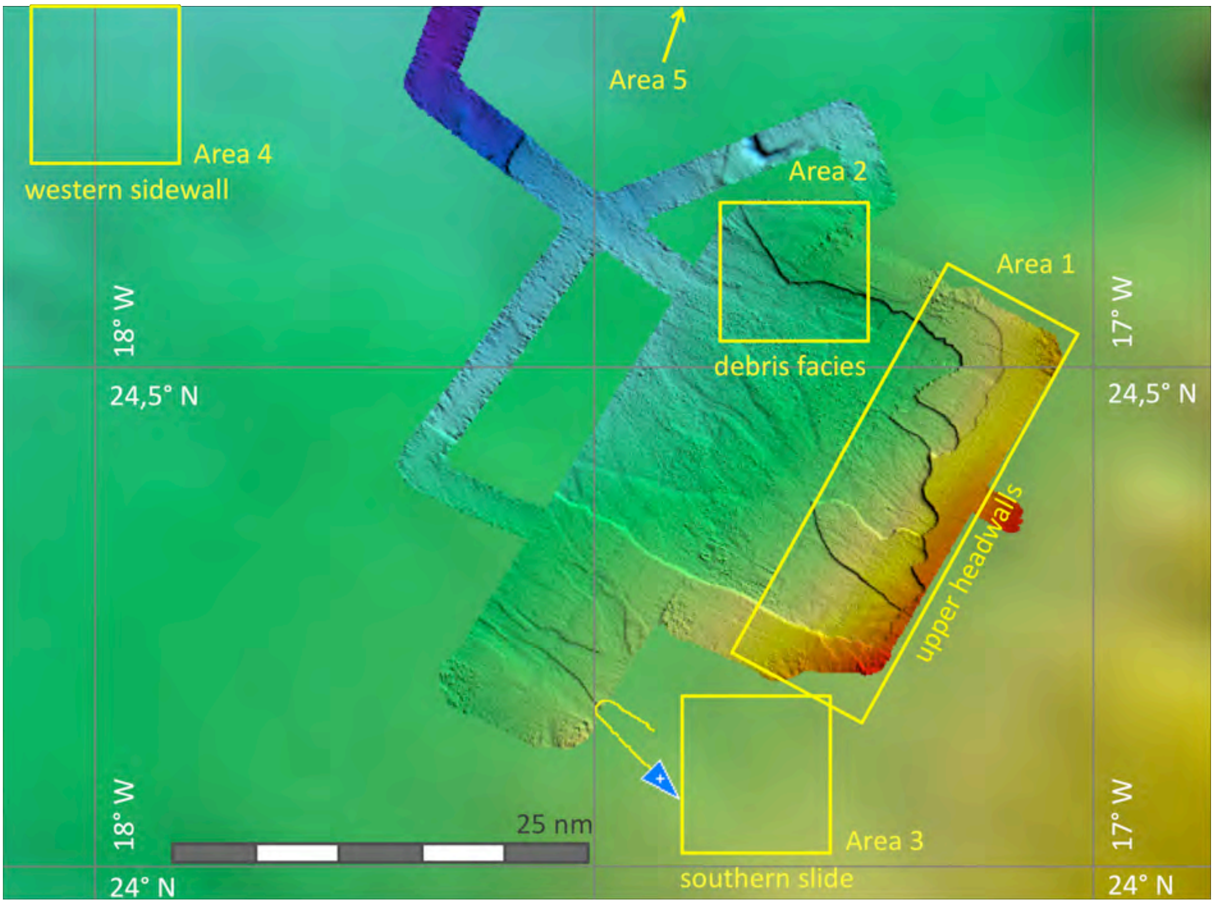

Fig. 29: Research area with target for station work (Area 1-5) on the Sahara Slide.

5.4.1. Sampling locations

Additional sampling areas were chosen on the different slide debris facies (Area 2) further west on the lateral boundaries of the Sahara Slide (Area 4), further north on the lateral boundaries of its distal deposits (Area 5) and further south on a smaller submarine slide (Area 3; Fig. 29). We applied the standard gravity corer equipped with a 5m barrel (Fig. 30).

However, due to problems with the stabilizing system of the vessel and increasing swell, a substantial part of the sedimentological sampling program (Areas 2-5) was cancelled.

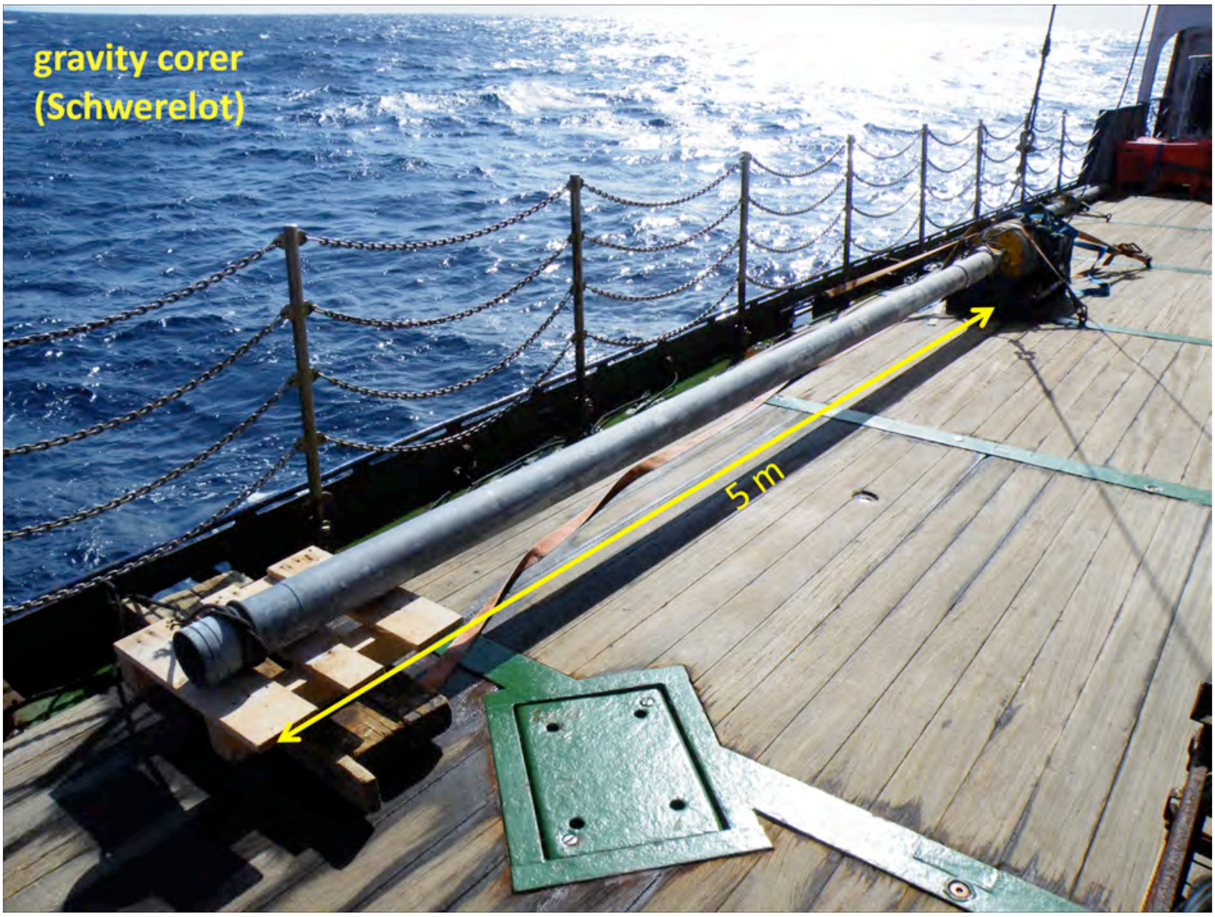

Fig. 30: The standard gravity corer equipped with a 5m barrel was applied at all stations.

5.4.2. First Results

The recovery varied drastically in the upper headwall area reaching from 4.8 m to nearly zero with some light grey, consolidated mud in the core catcher (**Fehler! Verweisquelle konnte nicht gefunden werden.**). The overall picture of sedimentary sequence in this area is consistent showing debris (clasts, debris flow deposits, incorporated blocks) on consolidated mud (Fig. 31). The later probably constitutes glide plane material (Fig. 32a). All these are capped by a distinct thin sedimentary drape of well-oxidised sediment (greyish-pink foram-bearing mud) that is interpreted as rather young Holocene deposit (Fig. 32b). Locations of recovered gravity cores are listed in Table 2.

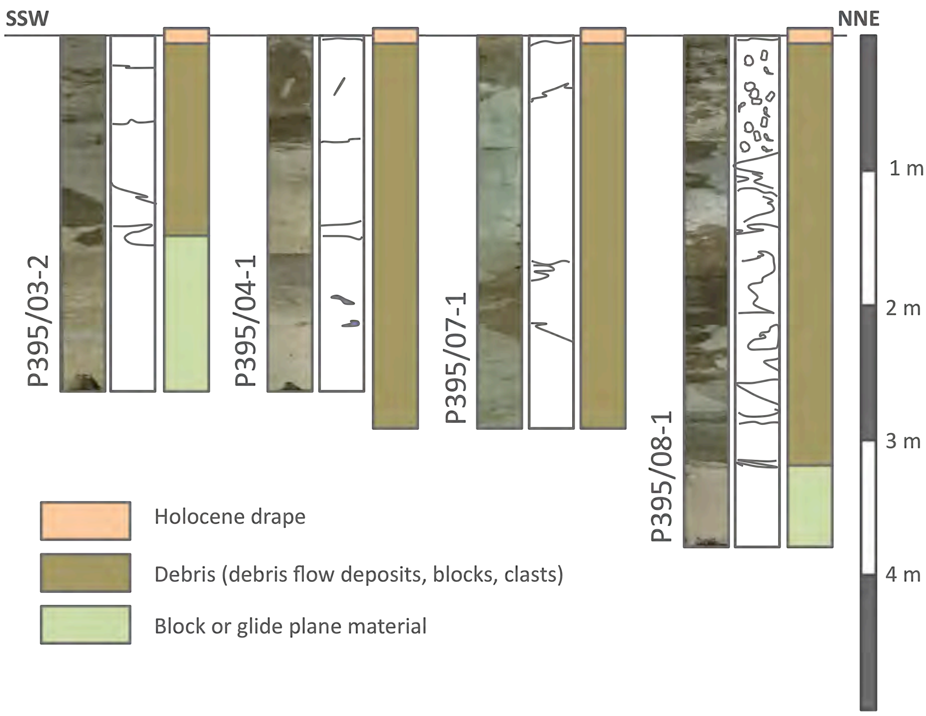

Fig. 31: Correlation of corers across the upper headwall showing a consistent picture of debris resting on glide plane material with a thin Holocene well-oxidised drape on top.

Fig. 32: Up: Core catcher of P395/10-1 contained consolidated, light grey mud probably representing glide plane material. Lower left: Split core segments of P395/08-1 showing the mosaic of mud clasts typical for debris flow deposits on larger tilted, sheared, deformed blocks of the same debris flow. Note the thin sedimentary drape of well-oxidised sediment (greyish-pink foram-bearing mud) that is interpreted as rather young Holocene deposit. This drape was synoptically detected in all cores (lower right).

5.5.Wildlife observation

During P395 cruise numerous animal species have been observed in vicinity of the vessel like whales or dolphins but also birds that were attracted by the vessel. Wildlife observations were documented by Russel B. Wynn from February 4th to 17th.

4-7 Feb (Passage south from Canary Islands to Sahara Slide headwall)

Small numbers (<50) of Cory's Shearwater (all borealis race), Manx Shearwater, Leach's Storm Petrel, Gannet (mostly immatures), Grey Phalarope, Arctic Skua and Kittiwake (mostly 1st-winters) noted. Two groups of Atlantic Spotted Dolphins were seen, including four that were photographed bow riding in association with large tuna. One flying fish was also seen.

8-17 Feb (Sahara Slide headwall region)

Water depths between 1500-2000 m; SST = 20°C

15 hours of observations; 4-40 seabirds per hour (daily average)

74 Cory's Shearwater (mostly moving N)

61 Arctic Skuas

55 Grey Phalaropes

29 Leach's Storm Petrels

10 Kittiwakes

5 White-faced Storm Petrels

3 Manx Shearwaters

2 Great Skuas

1 European Storm Petrel

1 Royal Tern

24 Bryde's Whales

50-100+ Common Dolphins

50-100+ Atlantic Spotted Dolphins

Fig. 33: Bryde`s Whale

8 Feb

During the morning a couple of Arctic Skuas were seen. Observations from ~1800-1900 hrs, in light winds, produced a single Bryde's Whale (photographed, Fig. 33), together with a loose multi-species foraging aggregation, comprising two Cory's Shearwaters, two Manx Shearwaters, two White-faced Storm Petrels, single Leach's and European Storm Petrels and two Grey Phalaropes. Baitfish could be seen boiling at the surface in the vicinity. A further distant rorqual blow was later observed in the distance. A Racing Pigeon and a small locust arrived on deck.

9 Feb

A White-faced Storm Petrel was captured in the lab and boxed overnight. It was photographed and released successfully at dawn. It was a mostly cloudy night with relatively light winds and the ship speed was 2-3 knots. The Racing Pigeon was still on board.

Observations from 1000-1100 hrs (wind – ENE 22 km/hr) produced 18 Cory's Shearwaters moving NW, four Arctic Skuas, two 1st-winter Kittiwakes and single Leach's and White-faced Storm Petrels. A group of 50-100 Common Dolphins approached the ship, despite seismic operations being in progress. **26 birds per hour (bph)**.

Observations from 1620-1720 hrs (wind – NE 25 km/hr) produced 13 Arctic Skuas mostly moving NNE, nine Cory's Shearwaters moving NNE, seven Leach's Storm Petrels loosely foraging together, three Grey Phalaropes, one Manx Shearwater and one 1st-winter Kittiwake. All Arctic Skuas were seen as singles flying high off the sea and occasionally dropping down to pick food items off the sea surface. They have yet to be seen pursuing other seabirds. No fishing boats yet recorded. **34 bph**.

10 Feb

A Leach's Storm Petrel was captured on deck and boxed overnight. It was photographed and released successfully at dawn. It was a breezy night with fairly clear skies and the ship was moving at 2-3 knots.

Observations from 0825-0925 hrs (wind – NE 32 km/hr) produced 30 Grey Phalaropes (including a flock of 25 sitting on the sea), three Cory's Shearwaters, three Arctic Skuas, one Leach's Storm Petrel, one adult Kittiwake (briefly following the ship, as those seen on previous days have been) and one Royal Tern. Another Racing Pigeon arrived on deck. Two rorqual blows were seen together, probably Bryde's Whales. **39 bph**.

Fig. 34: Cory`s Shearwater

Observations from 1500-1600 hrs (wind – NE 21 km/hr) produced 11 Cory's Shearwaters moving NE, 2 adult Kittiwakes and a Leach's Storm Petrel. Two separate rorqual blows were also seen (note that this survey was undertaken down slope of the upper slide headwall at water depth 2500 m). **14 bph**.

Fig. 35: Atlantic Spotted Dolphin

<u>11 Feb</u>

Observations from 0815-0915 hrs (wind – ENE 26 km/hr) pro Arctic Skuas, two Cory's Shearwaters and single 1st-winter faced Storm Petrels. Four distant rorqual blows were also seen

Observations from 1810-1850 hrs (wind – NNE 29 km/hr) pr well as a group of 50-100+ Atlantic Spotted Dolphins (Fig. 35) that were bow-riding for several minutes. **5 bph**.

<u>12 Feb</u>

Observations from 1755-1855 hrs (wind – NNE 15 km/hr) produced four Cory's Shearwaters, two Arctic Skuas and single Grey Phalarope and White-faced Storm Petrel. A Racing Pigeon also remained onboard. However, the highlight was three Bryde's Whales surface-feeding along a linear slick (generated by Langmuir circulation) within 200 m of the ship. They passed down the port side and didn't change behavior or direction even though we were running multi-channel seismics. A further rorqual blow was also seen distantly. **8 bph**.

Fig. 36: Leach`s Storm Petrel

<u>13 Feb</u>

Observations from 0825-0925 hrs (wind – NE 15 km/hr) produced three Leach's Storm Petrels and single Cory's Shearwater and Arctic Skua. Three rorqual blows were seen, with a brief view of one dorsal fin indicating a probable Bryde's Whale. **5 bp**.

Observations from 1200-1240 hrs (wind – NNE 5 km/hr) produced single Great Skua, Arctic Skua and Leach's Storm Petrel, as well as a single rorqual blow. **5 bph**.

Observations from 1730-1800 hrs (wind – WNW 10 km/hr) produced 19 Cory's Shearwaters moving NE, seven Arctic Skuas, three Leach's Storm Petrels, two Grey Phalaropes, one Great

Skua (see attacking Cory's Shearwater) and an adult and 1st-winter Kittiwake (attacked by Arctic Skua). A probable Bryde's Whale was also seen. **68 bph**.

14 Feb

Observations from 0845-0945 hrs (wind SSW – 30 km/hr) produced seven Grey Phalaropes, four Arctic Skuas, two Leach's Storm Petrels and a 1st-winter Kittiwake. Five rorqual blows were also seen. **28 bph**.

15 Feb

A Leach's Storm Petrel was captured on deck and boxed overnight, before being photographed and released at dawn (Fig. 36).

Observations from 0840-0910 hrs (wind WNW – 56 km/hr) produced just a single Arctic Skua. **2 bph**.

Observations from 1555-1655 hrs (wind – WNW 35 km/hr) produced eight Arctic Skuas and two Cory's Shearwaters. **10 bph**.

16 Feb

Observations from 0820-0920 hrs (wind W – 36 km/hr) produced two Leach's Storm Petrels and a single Cory's Shearwater. **3 bph**.

Observations from 1550-1650 hrs (wind WSW – 33 km/hr) produced three Leach's Storm Petrels, two Arctic Skuas and a Cory's Shearwater. **6 bph**.

17 Feb

Observations from 0845-0930 (wind SW – 42 km/hr) produced three Arctic Skuas and single Cory's Shearwater and Leach's Storm Petrel. **6 bph**.

6. Station List

Table 2: List of Seismic Profiles

Profil-Nr.	Date	Time Start UTC	Time End UTC	Latitude Start xx° xx.x'	Longitude Start xx° xx.x'	Latitude End xx° xx.x'	Longitude End xx° xx.x'
1	05.02.2010	20:40	04:23	24°20.40'	16°30.5'	24°23.00'	17°6.37'
2	06.02.2010	04:28	04:28	24°22.23'	17° 6.77'	24°23.00'	17° 6.37'
3	06.02.2010	04:56	06:26	24°24.21'	17°6.62'	24°28.21'	17° 12.39'
4	06.02.2010	06:30	06:48	24°28.34'	17° 12.27'	24°29.23'	17° 11.14'
5	06.02.2010	06:52	08:15	24° 29.12'	17° 10.82'	24°26.43'	17° 4.90'
6	06.02.2010	18:43	21:00	24° 32.77'	17° 3.13'	24°50.82'	17°22.85'
7	06.02.2010	21:01	22:01	24°30.49'	17°13.71'	24°26.97'	17°16.79'
8	07.02.2010	22:02	00:44	24°26.97'	17°16.79'	24°18.67'	17°7.63'
9	07.02.2010	00:47	01:28	24°18.67'	17°7.63'	24°15.86'	17°9.10'
10	07.02.2010	01:31	04:15	24°15.86'	17°9.10'	24° 23.02'	17° 19.16'
11	07.02.2010	04:19	05:24	24° 22.90'	17° 19.28'	24° 18.48'	17° 20.74'
12	07.02.2010	05:29	08:06	24° 18.35	17° 20.53	24°13.019'	17°9.56'
13	07.02.2010	08:09	08:50	24°12.9'	17°9.6'	24°10.45'	17°11.29'
14	07.02.2010	08:51	10:26	24°10.44'	17°11.35'	24°12.67'	17°17.88'
15	07.02.2010	13:01	13:41	24°8.22'	17°31.31'	24°10.13'	17°13.81'
16	07.02.2010	13:45	00:19	24°10.27'	17°13.77'	24°36.93'	17°2.4'
17	08.02.2010	02:05	12:40	24°35.82'	17°05.55'	24°9.20'	17°16.03'
18	08.02.2010	14:25	01:28	24°9.02'	17°13.48	24°36.49	17°1.81'
19	09.02.2010	03:33	13:41	24°34.00'	17°4.46'	24°7.72'	17°15.74'
20	09.02.2010	15:41	23:19	24°7.62'	17°13.17'	24°25.03'	17°5.89
21	10.02.2010	01:19	06:47	24°24.88'	17°10.13'	24°11.75	17°15.78'
22	10.02.2010	10:17	11:43	24°12.00'	17°16.58'	24°18.25'	17°18.99
23	10.02.2010	11:45	18:37	24°18.25'	17°18.99	24°42.16	17°44.87'
24	10.02.2010	18:41	20:07	24°42.29	17°44.71'	24°46.31	17°39.05'
25	10.02.2010	20:10	22:37	24°46.21	17°38.85	24°38.21'	17°29.31'
26	10.02.2010	22:38	04:45	24°38.21'	17°29.31'	24°7.86'	17°26.45'
27	11.02.2010	04:45	06:49	24°7.86'	17°26.45'	24°1.50'	17°19.99
28	11.02.2010	18:55	21:54	24°16.29'	17°6.52'	24°24.46	17°17.23
29	11.02.2010	21:58	22:42	24°24.46	17°17.23	24°26.74'	17°14.67'
30	11.02.2010	22:43	01:07	24°26.66'	17°14.55'	24°19.89'	17°05.52'
31	12.02.2010	01:11	01:39	24°20.05'	17°05.34'	24°21.68'	17°04.33'
32	12.02.2010	01:43	03:55	24°21.91'	17°04.51	24°28.02'	17°13.37'
33	12.02.2010	03:57	04:11	24°28.15'	17°13.39'	24°28.83	17°12.51'
34	12.02.2010	04:15	06:24	24°28.77	17°12.16'	24°23.63'	17°3.46'
35	12.02.2010	17:30	21:36	24°23.47'	17°10.74'	24°32.34'	17°7.14'
36	13.02.2010	00:48	11:02	24°36.02'	17°07.92'	24°12.35'	17°18.13'
37	14.02.2010	08:41	14:25	24°24.65'	17°13.70'	24°11.26'	17°19.59'
38	14.02.2010	16:37	03:54	24°12.88'	17°17.01'	24°37.79'	17°06.28'
39	15.02.2010	05:56	12:04	24°37.43'	17°09.09'	24°24.65'	17°41.59'
40	16.02.2010	10:15	13:34	24°9.02'	17°29.74'	23°59.68'	17°18.45'
41	16.02.2010	13:37	16:39	23°59.72'	17°18.25'	24°03.76'	17°05.82'
42	16.02.2010	16:43	23:18	24°03.76'	17°05.82'	24°28.37'	16°56.58'
43	16.02.2010	23:18	07:57	24°28.37'	16°56.58'	24°52.78°	17°21.14'

Table 3: List of sampling stations

Station	Lat	Lon	Depth (m)	Recovery (m)

P395/02-1	24° 27,05' N	17° 06,32' W	2033	5
P395/03-1	24° 13,22' N	17° 14,63' W	1873	0,36
P395/03-2	24° 13,21' N	17° 14,62' W	1883	2,55
P395/04-1	24° 14,70' N	17° 13,40' W	1930	2,57
P395/05-1	24° 16,09' N	17° 12,61' W	1971	0,35
P395/06-1	24° 18,79' N	17° 11,08' W	1999	0
P395/07-1	24° 37,36' N	17° 08,18' W	2132	4,8
P395/08-1	24° 26,35' N	17° 08,63' W	2157	3,78
P395/09-1	24° 25,43' N	17° 09,03' W	2144	1,37
P395/10-1	24° 20,93' N	17° 09,87' W	2039	0,25
P395/11-1	24° 20,57' N	17° 10,05' W	2036	2,77

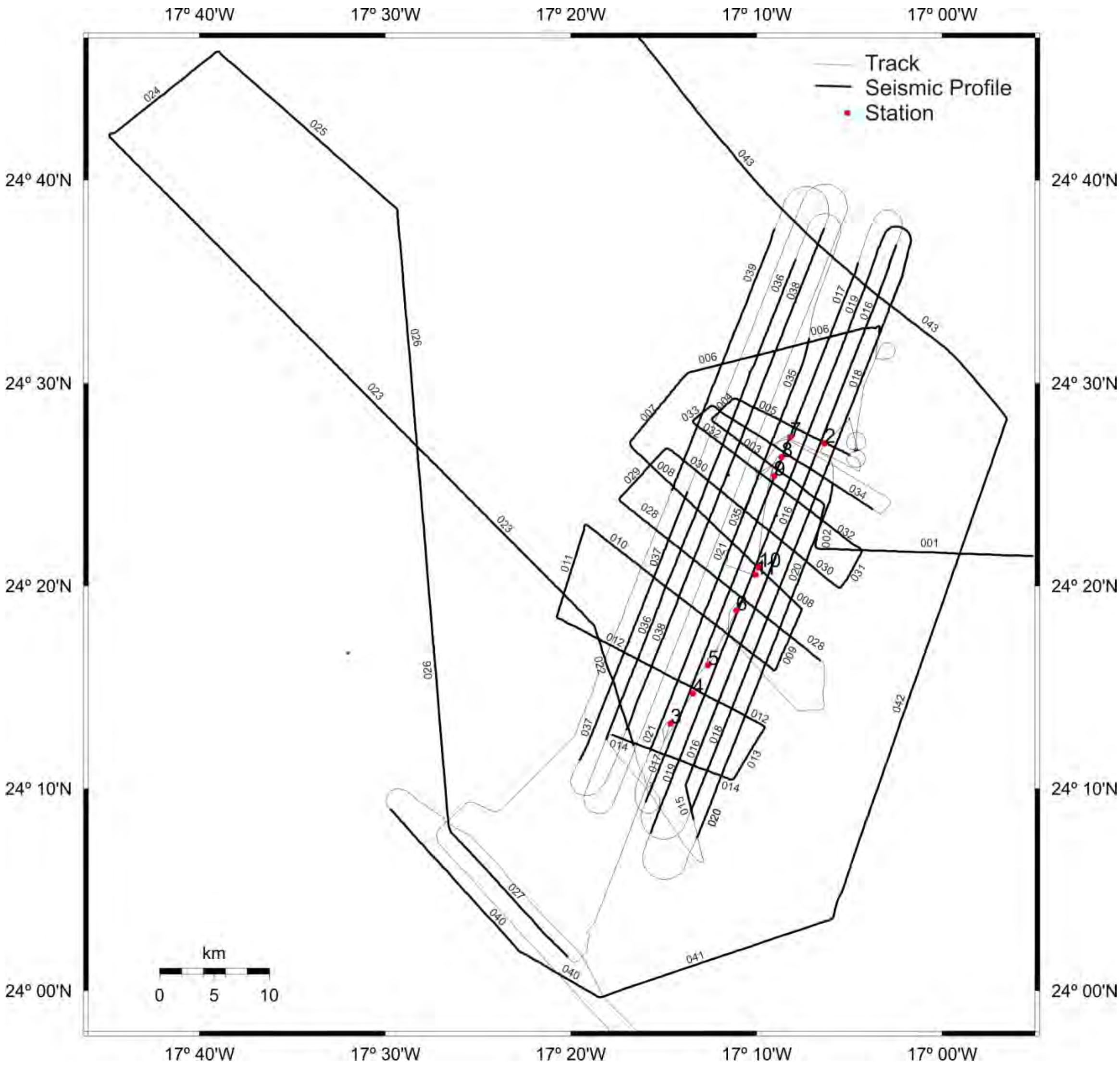

Fig. 37: Map of seismic profiles and coring stations

7. Data and Sample Storage and Availability

The collected sediment cores are archived in the core repository of IFM-GEOMAR in Kiel. The seismic and hydro-acoustic raw data as well as processed data will be archived on a dedicated server at IFM-GEOMAR, which is daily backed up.

8. Acknowledgement

The scientific party of Poseidon Cruise P395 gratefully acknowledges the very friendly and most effective cooperation with Captain Schneider and his crew. Their perfect technical assistance substantially contributed to make this cruise a scientific success. We also appreciate the valuable support of the IFM-GEOMAR ships coordination office. This expedition was funded by the Deutsche Forschungsgemeinschaft.

9. References

Blondel, P. & Murton, B.J., 1997. *Handbook of seafloor sonar imagery,* Wiley, 314 pp..

Embley, R.W., 1976. New evidence for occurrence of debris flow deposits in the deep sea. *Geology*, 4, 371-374.

Embley, R.W. & Jacobi, R.D., 1977. Distribution and morphology of large submarine sediment slides and slumps on Atlantic continental margins, *Marine Georesources & Geotechnology,* 2**,** 205-228.

Embley, R.W., 1982. Anatomy of some Atlantic margin sediment slides and some comments on ages and mechanisms, *Marine Slides and Other Mass Movements. Plenum Press, New York***,** 189–214.

Gee, M., Masson, D., Watts, A. & Allen, P., 1999. The Saharan debris£ ow: an insight into the mechanics of long runout submarine debris£ ows, *Sedimentology,* 46, 317-335.

Georgiopoulou, A., Krastel, S., Masson, D.G. & Wynn, R.B., 2007. Repeated instability of the NW African margin related to buried landslide scarps, *Submarine Mass Movements and Their Consequences***,** 29-36.

Georgiopoulou, A., Wynn, R.B., Masson, D.G. & Frenz, M., 2009. Linked turbidite-debrite resulting from recent Sahara Slide headwall reactivation, *Marine and Petroleum Geology,* 26**,** 2021-2031.

Hayes, D.E. & Rabinowitz, P.D., 1975. Mesozoic magnetic lineations and the magnetic quiet zone off northwest Africa, *Earth and Planetary Science Letters,* 28**,** 105-115.

Johnson, H.P. & Helferty, M., 1990. The geological interpretation of side-scan sonar, *Reviews of Geophysics,* 28**,** 357-380.

Klaucke, I., Sahling, H., Weinrebe, W., Blinova, V., Bürk, D., Lursmanashvili, N. & Bohrmann, G., 2006. Acoustic investigation of cold seeps offshore Georgia, Eastern Black Sea, *Marine Geology*, 231, 51-67.

Klaucke, I., Weinrebe, W., Petersen, C.J. & Bowden, D., 2010. Temporal variability of gas seeps offshore New Zealand: Multi-frequency geoacoustic imaging of the Wairarapa area, Hikurangi margin, *Marine Geology,* 272**,** 49-58.

Krastel, S., Wynn, R.B., Honebuth, T., Henrich, R., Holz, C., Meggers, H., Kuhlmann, H., Georgiopoulou, A. & Schulz, H.D., 2006. Mapping of seabed morphology and shallow sediment structure of the Mauritania continental margin, Northwest Africa: some implications for geohazard potential, *Norwegian Journal of Geology,* 86**,** 163-176.

Masson, D.G., Kidd, R.B., Gardner, J.V., Huggett, Q.J. & Weaver, P.P.E., 1992. Saharan continental rise: facies distribution and sediment slides, *Geologic evolution of Atlantic continental rises*, 327-343.

Masson, D.G., Huggett, Q.J. & Brunsden, D, 1993. The surface texture of the Saharan Debris Flow deposit and some speculations on submarine debris flow processes. *Sedimentology,* 40, 583-598.

Masson, D.G., 1994. Late Quaternary turbidity current pathways to the Madeira Abyssal Plain and some constraints on turbidity current mechanisms, *Basin Research,* 6**,** 17-33.

Masson, D.G., Watts, A., Gee, M., Urgeles, R., Mitchell, N., Le Bas, T. & Canals, M., 2002. Slope failures on the flanks of the western Canary Islands, *Earth-Science Reviews,* 57**,** 1-35.

Mitchell, N.C., 1993. A model for attenuation of backscatter due to sediment accumulations and its application to determine sediment thicknesses with GLORIA sidescan sonar, *Journal of Geophysical Research,* 98**,** 22477-22422,22493.

Weaver, P.P.E., Wynn, R.B., Kenyon, N.H. & Evans, J., 2000. Continental margin sedimentation, with special reference to the north east Atlantic margin, *Sedimentology,* 47**,** 239-256.

Wynn, R.B., Masson, D.G., Stow, D.A.V. & Weaver, P.P.E., 2000. Turbidity current sediment waves on the submarine slopes of the western Canary Islands, *Marine Geology,* 163**,** 185-198.

Wynn, R.B., Weaver, P.P.E., Masson, D.G. & Stow, D.A.V., 2002. Turbidite depositional architecture across three interconnected deep water basins on the north west African margin, *Sedimentology,* 49**,** 669-695.

IFM-GEOMAR
Leibniz-Institut für Meereswissenschaften
an der Universität Kiel

IFM-GEOMAR Reports

No.	Title
1	RV Sonne Fahrtbericht / Cruise Report SO176 & 179 MERAMEX I & II (Merapi Amphibious Experiment) 18.05.-01.06.04 & 16.09.-07.10.04. Ed. by Heidrun Kopp & Ernst R. Flueh, 2004, 206 pp. In English
2	RV Sonne Fahrtbericht / Cruise Report SO181 TIPTEQ (from The Incoming Plate to mega Thrust EarthQuakes) 06.12.2004.-26.02.2005. Ed. by Ernst R. Flueh & Ingo Grevemeyer, 2005, 533 pp. In English
3	RV Poseidon Fahrtbericht / Cruise Report POS 316 Carbonate Mounds and Aphotic Corals in the NE-Atlantic 03.08.–17.08.2004. Ed. by Olaf Pfannkuche & Christine Utecht, 2005, 64 pp. In English
4	RV Sonne Fahrtbericht / Cruise Report SO177 - (Sino-German Cooperative Project, South China Sea: Distribution, Formation and Effect of Methane & Gas Hydrate on the Environment) 02.06.-20.07.2004. Ed. by Erwin Suess, Yongyang Huang, Nengyou Wu, Xiqiu Han & Xin Su, 2005, 154 pp. In English and Chinese
5	RV Sonne Fahrtbericht / Cruise Report SO186 – GITEWS (German Indonesian Tsunami Early Warning System 28.10.-13.1.2005 & 15.11.-28.11.2005 & 07.01.-20.01.2006. Ed. by Ernst R. Flueh, Tilo Schoene & Wilhelm Weinrebe, 2006, 169 pp. In English
6	RV Sonne Fahrtbericht / Cruise Report SO186 -3 – SeaCause II, 26.02.-16.03.2006. Ed. by Heidrun Kopp & Ernst R. Flueh, 2006, 174 pp. In English
7	RV Meteor, Fahrtbericht / Cruise Report M67/1 CHILE-MARGIN-SURVEY 20.02.-13.03.2006. Ed. by Wilhelm Weinrebe und Silke Schenk, 2006, 112 pp. In English
8	RV Sonne Fahrtbericht / Cruise Report SO190 - SINDBAD (Seismic and Geoacoustic Investigations Along The Sunda-Banda Arc Transition) 10.11.2006 - 24.12.2006. Ed. by Heidrun Kopp & Ernst R. Flueh, 2006, 193 pp. In English
9	RV Sonne Fahrtbericht / Cruise Report SO191 - New Vents "Puaretanga Hou" 11.01. - 23.03.2007. Ed. by Jörg Bialas, Jens Greinert, Peter Linke, Olaf Pfannkuche, 2007, 190 pp. In English
10	FS ALKOR Fahrtbericht / Cruise Report AL 275 - Geobiological investigations and sampling of aphotic coral reef ecosystems in the NE-Skagerrak, 24.03. - 30.03.2006, Eds.: Andres Rüggeberg & Armin Form, 39 pp. In English

IFM-GEOMAR
Leibniz-Institut für Meereswissenschaften
an der Universität Kiel

No.	Title
11	FS Sonne / Fahrtbericht / Cruise Report SO192-1: MANGO: Marine Geoscientific Investigations on the Input and Output of the Kermadec Subduction Zone, 24.03. - 22.04.2007, Ernst Flüh & Heidrun Kopp, 127 pp. In English
12	FS Maria S. Merian / Fahrtbericht / Cruise Report MSM 04-2: Seismic Wide-Angle Profiles, Fort-de-France – Fort-de-France, 03.01. - 19.01.2007, Ed.: Ernst Flüh, 45 pp. In English
13	FS Sonne / Fahrtbericht / Cruise Report SO193: MANIHIKI Temporal, Spatial, and Tectonic Evolution of Oceanic Plateaus, Suva/Fiji – Apia/Samoa 19.05. - 30.06.2007, Eds.: Reinhard Werner and Folkmar Hauff, 201 pp. In English
14	FS Sonne / Fahrtbericht / Cruise Report SO195: TOTAL TOnga Thrust earthquake Asperity at Louisville Ridge, Suva/Fiji – Suva/Fiji 07.01. - 16.02.2008, Eds.: Ingo Grevemeyer & Ernst R. Flüh, 106 pp. In English
15	RV Poseidon Fahrtbericht / Cruise Report P362-2: West Nile Delta Mud Volcanoes, Piräus – Heraklion 09.02. - 25.02.2008, Ed.: Thomas Feseker, 63 pp. In English
16	RV Poseidon Fahrtbericht / Cruise Report P347: Mauritanian Upwelling and Mixing Process Study (MUMP), Las-Palmas - Las Palmas, 18.01. - 05.02.2007, Ed.: Marcus Dengler et al., 34 pp. In English
17	FS Maria S. Merian Fahrtbericht / Cruise Report MSM 04-1: Meridional Overturning Variability Experiment (MOVE 2006), Fort de France – Fort de France, 02.12. – 21.12.2006, Ed.: Thomas J. Müller, 41 pp. In English
18	FS Poseidon Fahrtbericht /Cruise Report P348: SOPRAN: Mauritanian Upwelling Study 2007, Las Palmas - Las Palmas, 08.02. - 26.02.2007, Ed.: Hermann W. Bange, 42 pp. In English
19	R/V L'ATALANTE Fahrtbericht / Cruise Report IFM-GEOMAR-4: Circulation and Oxygen Distribution in the Tropical Atlantic, Mindelo/Cape Verde - Mindelo/Cape Verde, 23.02. - 15. 03.2008, Ed.: Peter Brandt, 65 pp. In English
20	RRS JAMES COOK Fahrtbericht / Cruise Report JC23-A & B: CHILE-MARGIN-SURVEY, OFEG Barter Cruise with SFB 574, 03.03.-25.03. 2008 Valparaiso – Valparaiso, 26.03.-18.04.2008 Valparaiso - Valparaiso, Eds.: Ernst Flüh & Jörg Bialas, 242 pp. In English
21	FS Poseidon Fahrtbericht / Cruise Report P340 – TYMAS "Tyrrhenische Massivsulfide", Messina – Messina, 06.07.-17.07.2006, Eds.: Sven Petersen and Thomas Monecke, 77 pp. In English

No.	Title
22	RV Atalante Fahrtbericht / Cruise Report HYDROMAR V (replacement of cruise MSM06/2), Toulon, France - Recife, Brazil, 04.12.2007 - 02.01.2008, Ed.: Sven Petersen, 103 pp. In English
23	RV Atalante Fahrtbericht / Cruise Report MARSUED IV (replacement of MSM06/3), Recife, Brazil - Dakar, Senegal, 07.01. - 31.01.2008, Ed.: Colin Devey, 126 pp. In English
24	RV Poseidon Fahrtbericht / Cruise Report P376 ABYSS Test, Las Palmas - Las Palmas, 10.11. - 03.12.2008, Eds.: Colin Devey and Sven Petersen, 36 pp, In English
25	RV SONNE Fahrtbericht / Cruise Report SO 199 CHRISP Christmas Island Seamount Province and the Investigator Ridge: Age and Causes of Intraplate Volcanism and Geodynamic Evolution of the south-eastern Indian Ocean, Merak/Indonesia – Singapore, 02.08.2008 - 22.09.2008, Eds.: Reinhard Werner, Folkmar Hauff and Kaj Hoernle, 210 pp. In English
26	RV POSEIDON Fahrtbericht / Cruise Report P350: Internal wave and mixing processes studied by contemporaneous hydrographic, current, and seismic measurements, Funchal – Lissabon, 26.04.-10.05.2007 Ed.: Gerd Krahmann, 32 pp. In English
27	RV PELAGIA Fahrtbericht / Cruise Report Cruise 64PE298: West Nile Delta Project Cruise - WND-3, Heraklion - Port Said, 07.11.-25.11.2008, Eds.: Jörg Bialas & Warner Brueckmann, 64 pp. In English
28	FS POSEIDON Fahrtbericht / Cruise Report P379/1: Vulkanismus im Karibik-Kanaren-Korridor (ViKKi), Las Palmas – Mindelo, 25.01.-12.02.2009, Ed.: Svend Duggen, 74 pp. In English
29	FS POSEIDON Fahrtbericht / Cruise Report P379/2: Mid-Atlantic-Researcher Ridge Volcanism (MARRVi), Mindelo- Fort-de-France, 15.02.-08.03.2009, Ed.: Svend Duggen, 80 pp. In English
30	FS METEOR Fahrtbericht / Cruise Report M73/2: Shallow drilling of hydrothermal sites in the Tyrrhenian Sea (PALINDRILL), Genoa – Heraklion, 14.08.2007 – 30.08.2007, Eds.: Sven Petersen & Thomas Monecke, 235 pp. In English
31	FS POSEIDON Fahrtbericht / Cruise Report P388: West Nile Delta Project - WND-4, Valetta – Valetta, 13.07. - 04.08.2009, Eds.: Jörg Bialas & Warner Brückmann, 65 pp. In English
32	FS SONNE Fahrtbericht / Cruise Report SO201-1b: KALMAR (Kurile-Kamchatka and ALeutian MARginal Sea-Island Arc Systems): Geodynamic and Climate Interaction in Space and Time, Yokohama, Japan - Tomakomai, Japan, 10.06. - 06.07.2009, Eds.: Reinhard Werner & Folkmar Hauff, 105 pp. In English
33	FS SONNE Fahrtbericht / Cruise Report SO203: WOODLARK Magma genesis, tectonics and hydrothermalism in the Woodlark Basin, Townsville, Australia - Auckland, New Zealand 27.10. - 06.12.2009, Ed.: Colin Devey, 177 pp. In English

No.	Title
34	FS MARIA S. MERIAN Fahrtbericht / Cruise Report MSM 03-2: HYDROMAR IV: The 3rd dimension of the Logatchev hydrothermal field, Fort-de-France - Fort-de-France, 08.11. - 30.11.2006, Ed.: Sven Petersen, 98 pp. In English
35	FS SONNE Fahrtbericht / Cruise Report SO201-2 **KALMAR: K**urile-Kamchatka and **AL**eutian **MAR**ginal Sea-Island Arc Systems: Geodynamic and Climate Interaction in Space and Time Busan/Korea – Tomakomai/Japan, 30.08. - 08.10.2009, Eds.: Wolf-Christian Dullo, Boris Baranov, and Christel van den Bogaard, 233 pp. In English
36	RV CELTIC EXPLORER Fahrtbericht / Cruise Report CE0913: Fluid and gas seepage in the North Sea, Bremerhaven – Bremerhaven, 26.07. - 14.08.2009, Eds.: Peter Linke, Mark Schmidt, CE0913 cruise participants, 90 pp. In English
37	FS SONNE Fahrtbericht / Cruise Report: TransBrom SONNE, Tomakomai, Japan - Townsville, Australia, 09.10. - 24.10.2009, Eds.: Birgit Quack & Kirstin Krüger, 84 pp. In English
38	FS POSEIDON Fahrtbericht / Cruise Report POS403, Ponta Delgada (Azores) - Ponta Delgada (Azores), 14.08. - 30.08.2010, Eds.: Torsten Kanzow, Andreas Thurnherr, Klas Lackschewitz, Marcel Rothenbeck, Uwe Koy, Christopher Zappa, Jan Sticklus, Nico Augustin, 66 pp. In English
39	FS SONNE Fahrtbericht/Cruise Report SO208 Leg 1 & 2 Propagation of Galápagos Plume Material in the Equatorial East Pacific (PLUMEFLUX), Caldera/Costa Rica – Guayaquil/Ecuador 15.07. - 29.08.2010, Eds.: Reinhard Werner, Folkmar Hauff and Kaj Hoernle, 230 pp, In English
40	Expedition Report "Glider fleet", Mindelo (São Vincente), Republic of Cape Verde, 05. – 19.03.2010, Ed.: Torsten Kanzow, 26 pp, In English
41	FS SONNE Fahrtbericht / Cruise Report SO206, Caldera, Costa Rica – Caldera, Costa Rica, 30.05. – 19.06.2010, Ed.: Christian Hensen, 95 pp, In English
42	FS SONNE Fahrtbericht / Cruise Report SO212, Talcahuano, Chile – Valparaiso, Chile, 22.12. – 26.12.2010, Ed.: Ernst Flüh, 47 pp, in English
43	RV Chakratong Tongyai Fahrtbericht / Cruise Report MASS-III, Morphodynamics and Slope Stability of the Andaman Sea Shelf Break (Thailand), Phuket - Phuket (Thailand), 11.01. - 24.01.2011, Ed.: Sebastian Krastel, 42 pp, in English.
44	FS SONNE Fahrtbericht / Cruise Report SO210, Identification and investigation of fluid flux, mass wasting and sediments in the forearc of the central Chilean subduction zone (ChiFlux), Valparaiso – Valparaiso, 23.09. – 01.11.2010, Ed.: Peter Linke, 112 pp, in English.
45	RV Poseidon POS389 & POS393 & RV Maria S. Merian MSM15/5, TOPO-MED - Topographic, structural and seismotectonic consequences of plate re-organization in the Gulf of Cadiz and Alboran Sea – POS 389: Valletta, Malta – Malaga, Spain, 06.–17.08.2009, POS393: Malaga, Spain – Faro, Portugal, 14.–24.01.2010, MSM15/5: Valletta, Malta - Rostock, Germany, 17.–29.07.2010, I. Grevemeyer, 52 pp.

No.	Title
46	FS POSEIDON Fahrtbericht / Cruise Report, P408 - The Jeddah Transect, Jeddah - Jeddah, Saudi Arabia, 13.01.–02.03.2011, M. Schmidt, C. Devey, A. Eisenhauer and cruise participants, 80 pp.
47	FS SONNE Fahrtbericht / Cruise Report, SO214 NEMESYS, Wellington – Wellington, 09.03. - 05.04.2011, Wellington - Auckland 06. - 22.04.2011, Ed.: J. Bialas, 174 pp.
48	FS POSEIDON Fahrtbericht / Cruise Report, P399 - 2&3, Las Palmas - Las Palmas (Canary Islands), 31.05.2010 – 17.06.2010 & Las Palmas (Canary Islands), Vigo (Spain), 18. – 24.06.2010, Ed.: H. Bange, 84 pp.
49	RV AEGAEO Fahrtbericht / Cruise Report, West Nile Delta Project Cruise - WND-V, 15.06. – 25.06.2010, Heraklion- Heraklion (Greece), Ed.: W. Brückmann, 51 pp.

IFM-GEOMAR

Leibniz-Institut für Meereswissenschaften
an der Universität Kiel

Das Leibniz-Institut für Meereswissenschaften ist ein Institut der Wissenschaftsgemeinschaft Gottfried Wilhelm Leibniz (WGL)

The Leibniz-Institute of Marine Sciences is a member of the Leibniz Association (Wissenschaftsgemeinschaft Gottfried Wilhelm Leibniz).

Leibniz-Institut für Meereswissenschaften / Leibniz-Institute of Marine Sciences
IFM-GEOMAR
Dienstgebäude Westufer / West Shore Building
Düsternbrooker Weg 20
D-24105 Kiel
Germany

Leibniz-Institut für Meereswissenschaften / Leibniz-Institute of Marine Sciences
IFM-GEOMAR
Dienstgebäude Ostufer / East Shore Building
Wischhofstr. 1-3
D-24148 Kiel
Germany

Tel.: ++49 431 600-0
Fax: ++49 431 600-2805
www.ifm-geomar.de